iScience

CellPress
OPEN ACCESS

Article

Circ_0007432 promotes non-small cell lung cancer progression and macrophage M2 polarization through SRSF1/KLF12 axis

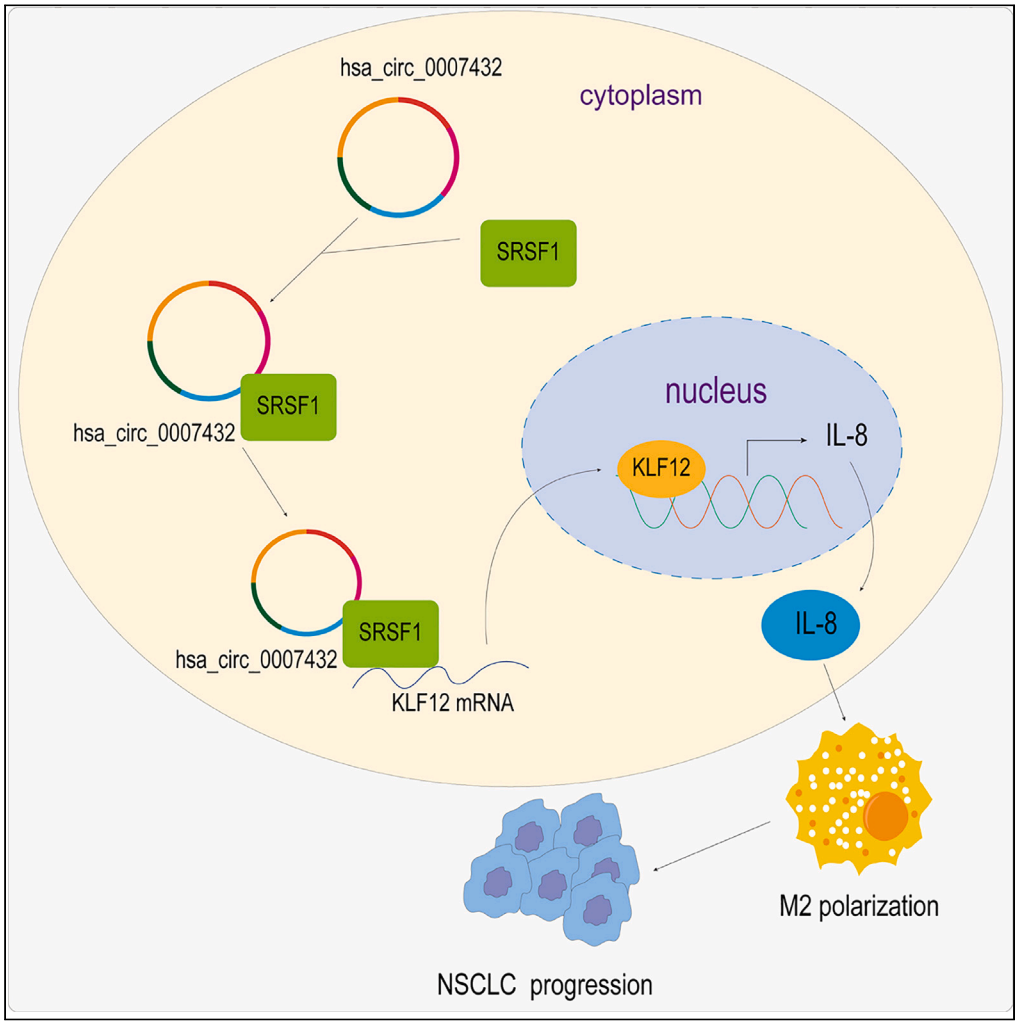

Shanshan Mao, Dongyu Wu, Xiaozhen Cheng, Jinsheng Wu

wjs7911@126.com

Highlights

Circ_0007432 knockdown suppressed malignant behaviors of NSCLC cells

Circ_0007432 promote KLF12 mRNA stability through interacting with SRSF1

KLF12 transcriptionally activated IL-8

Circ_0007432 elevated KLF12 to promote malignant behaviors of NSCLC cells

Circ_0007432 promoted M2 macrophage polarization by elevating KLF12 and IL-8

Mao et al., iScience 27, 109861
June 21, 2024
https://doi.org/10.1016/j.isci.2024.109861

iScience

CellPress
OPEN ACCESS

Article

Circ_0007432 promotes non-small cell lung cancer progression and macrophage M2 polarization through SRSF1/KLF12 axis

Shanshan Mao,[1,2] Dongyu Wu,[1] Xiaozhen Cheng,[2] and Jinsheng Wu[1,3,*]

SUMMARY

Circular RNAs (circRNAs) plays critical roles in non-small cell lung cancer (NSCLC) development. Herein, we illustrated the effects of circ_0007432 on malignant features of NSCLC. We found that circ_0007432 played a promoting role in NSCLC progression, lying in accelerating cell viability, migration and invasion of NSCLC cells, promoting M2 macrophage polarization, suppressing cell apoptosis of NSCLC cells, and enhancing tumor growth *in vivo*. Mechanistically, the interactions among circ_0007432, SRSF1, KLF12, and IL-8 were validated by RNA-binding protein immunoprecipitation (RIP), electrophoretic mobility shift assay (EMSA), RNA pull-down, dual luciferase reporter assay and chromatin immunoprecipitation (ChIP) assays. Circ_0007432 upregulated KLF12 by recruiting SRSF1. KLF12 facilitated IL-8 expression and release by binding to IL-8 promoter. Furthermore, the role of circ_0007432/SRSF1/KLF12/IL-8 axis in malignant phenotypes of tumor cells or macrophage polarization was investigated using rescue experiments. In conclusion, circ_0007432 bound with SRSF1 to stabilize KLF12 and then promote IL-8 release, thus promoting malignant behaviors of NSCLC cells and M2 macrophage polarization.

INTRODUCTION

Non-small cell lung cancer (NSCLC) with high incidence and mortality is one of the most common malignant tumors, accounting for roughly 85% of lung cancers.[1,2] At present, various therapies including surgery, chemoradiotherapy, targeted therapy, and immunotherapy have improved the prognosis of patients with NSCLC; however, therapeutic effects are still unsatisfactory.[3] There were studies supporting that targeted therapies have greatly improved outcomes for NSCLC patients.[4] Therefore, the search for more effective biomarkers and therapeutic targets may provide greater possibility for inhibiting the progression of NSCLC and improving the prognosis.

The tumor microenvironment (TME) is a complex system involving a variety of cellular and extracellular components that contribute to the tumorigenesis process.[5] Tumor-associated macrophages (TAMs) are immune cells in the tumor stroma microenvironment and have received increasing attention in mediating tumor progression.[6] Macrophages are highly plastic and heterogeneous, and could be polarized into M1 macrophages and M2 macrophages under different microenvironments.[7] Studies have shown that TAMs, manifested as M2 type in tumors and promoted extracellular matrix remodeling, tumor growth, and immunosuppression, contribute to poor prognosis in patients.[8–10] Therefore, exploring the mechanism of M2-type polarization in macrophages for NSCLC is essential.

Circular RNAs (circRNAs), structured by a closed loop, are important members of non-coding RNAs.[11] Massive investigations have determined that circRNAs are implicated in mediating tumor proliferation, invasion, and apoptosis of multiple human malignancies including NSCLC.[12,13] For example, circRNA OXCT1, circ_0008003, and circ_0001715 were reported to be closely related with NSCLC progression.[14–16] Circ_0007432 is derived from exons 3–7 of the PMM2 gene on chromosome 16, with a length of 461 bp. Ming-Ming Jiang and co-workers reported that circ_0007432 expression was abnormally elevated in three tissue samples from NSCLC patients, which was determined by human circular RNA microarray,[17] indicating circ_0007432 might be related with NSCLC progression. However, the effects and detailed mechanism of circ_0007432 in NSCLC are still unclear.

Krupple-like factor 12 (KLF12), belonging to KLF family, was implicated in malignant phenotypes of tumor cells.[18,19] Accumulating evidence revealed that KLF12 was abnormally expressed in various tumors including NSCLC.[20,21] KLF12 was highly expressed in tumor tissues of lung adenocarcinoma (a type of NSCLC) patients and KLF12 was regulated by lncRNA DARS-AS1/miR-188-5p axis to mediate lung adenocarcinoma cell growth and epithelial to mesenchymal transition (EMT) process,[20] suggesting that KLF12 probably plays a crucial role in NSCLC. Of note, JASPAR database predicted that KLF12 had a binding site on interleukin-8 (IL-8) promoter. IL-8, a cytokine in chemokines, was involved in regulating physiological and pathological processes. Some evidences have confirmed that IL-8 promoted the polarization of

[1]Radiotherapy Department, The First Affiliated Hospital of Hainan Medical University, Haikou 570102, Hainan Province, P.R. China
[2]Department of Medical Oncology, Haikou People's Hospital, Haikou 570208, Hainan Province, P.R. China
[3]Lead contact
*Correspondence: wjs7911@126.com
https://doi.org/10.1016/j.isci.2024.109861

macrophages into M2-type macrophages and participated in cancer progression.[22,23] In addition, IL-8 was reported to be engaged in lung cancer cell proliferation and metastasis.[24] Therefore, we put forward a conjecture: does KLF12 affect NSCLC progression and M2 macrophage polarization by regulating IL-8 expression?

Based on the background, we hypothesized that circ_0007432 might positively regulate KLF12 expression to increase IL-8 release, thus mediating cell growth of NSCLC and M2 macrophage polarization in TME.

RESULTS

High circ_0007432 expression was observed in NSCLC tissues and cells

Growing studies have found the important role of circRNAs in cancers. Previous studies have found a large number of circRNAs that are differentially expressed in NSCLC and normal cells.[17] Here, we selected 7 kinds of circRNAs with obvious changes for detection. Our results showed that circ_0007432 upregulation was most pronounced in NSCLC compared to para-carcinoma tissues (Figure S1). Subsequently, we evaluated the features of circ_0007432. As presented in Figure 1A, circ_0007432 is back-spliced from 5 exons (exons 3–7) of the PMM2 gene and the loop structure was determined by Sanger sequencing. RNase R digestion assay displayed that PMM2 was evidently decreased in H1975 and A549 cells after RNase R treatment, while circ_0007432 remained unchangeable (Figure 1B). In addition, circ_0007432 was more stable than PMM2 mRNA following actinomycin D (a transcription inhibitor) treatment (Figure 1C). Then, we analyzed the expression of circ_0007432 in 50 NSCLC patients, and the patient characteristics were summarized as shown in Table 1. Additionally, higher expression of circ_0007432 was observed in tumor tissues of NSCLC patients compared with para-carcinoma tissues (n = 50) (Figure 1D). Kaplan-Meier analysis suggested that higher expression of circ_0007432 contributed to poor prognosis of NSCLC patients (Figure 1E). Furthermore, circ_0007432 was preferentially located in the cytoplasm, which was determined by FISH and nucleoplasmic separation assays (Figures 1F and 1G). Finally, we found that circ_0007432 expression was also elevated in NSCLC cells including PC-9, Calu-3, H1975, A549, and H358, compared to human bronchial epithelial cells (BEAS-2B) (Figure 1H). Of note, due to highest circ_0007432 expression in H1975 and A549 cells, these two cell lines were used for subsequent experiments.

Circ_0007432 silencing suppressed malignant phenotypes of NSCLC

To investigate whether circ_0007432 mediates malignant behaviors of NSCLC cells, circ_0007432 was silenced in H1975 and A549 cells using sh-circ_0007432 transfection. RT-qPCR revealed high knockdown efficiency of sh-circ_0007432 transfection (Figure 2A). Cell viability was apparently suppressed by circ_0007432 knockdown (Figure 2B). In addition, circ_0007432 knockdown evidently promoted cell apoptosis (Figure 2C). Meantime, circ_0007432 knockdown resulted in elevation of Bax (a pro-apoptotic protein) and reduction of Bcl-2 (an anti-apoptotic protein) (Figure 2D). Moreover, circ_0007432 silencing resulted in suppression of cell migration and invasion, which was detected by wound healing and transwell test (Figures 2E and 2F). Altogether, circ_0007432 promoted cell growth of NSCLC cells.

Circ_0007432 maintained KLF12 mRNA stability by recruiting SRSF1

Here, KLF12 expression was detected in collected tumor tissues from 50 NSCLC patients. The results exhibited that KLF12 was highly expressed in tumor tissues in relative to para-carcinoma tissues (Figure 3A). In NSCLC, Pearson correlation analysis revealed a positive relationship between circ_0007432 and KLF12 expression (Figure 3B). KLF12 mRNA and protein expression was enhanced in NSCLC cells (Figures 3C and 3D). Circ_0007432 knockdown led to decreased KLF12 expression (Figures 3E and 3F). The mRNA stability of KLF12 was attenuated by circ_0007432 knockdown upon actinomycin D treatment (Figure 3G). Moreover, we conducted Ago2-RNA-binding protein immunoprecipitation (RIP) experiment to test whether circ_0007432 sponges miRNA, and the results showed that Ago2 failed to enrich circ_0007432 (Figure 3H), indicating that circ_0007432 might not have the function of "miRNA sponge" in H1975 and A549 cells. Therefore, we conjectured that circ_0007432 probably functions by binding to RNA binding proteins. RNA pull-down assay discovered that circ_0007432 probe could enrich SRSF1 protein, whereas scramble probe was unable to enrich SRSF1 protein (Figure 3I). Similarly, RNA-EMSA assay displayed that biotin-labeled circ_0007432 probe successfully pulled down SRSF1 (Figure S2A), indicating the interaction between circ_0007432 and SRSF1. Furthermore, the detailed region of SRSF1 binding to circ_0007432 was validated. SRSF1 is known to consist of an RS domain and two RNA recognition motifs (RRMs) responsible for specific interactions with RNA.[25] To identify the domain where SRSF1 binds to circ_0007432, we constructed a series of SRSF1 domain mutants (Figure S2B) and then we transfected 293T cells with the aforementioned vectors and flag-tagged circ_0007432. Using RIP detection, we validated that circ_0007432 was bound to RRM1 and RRM2 at the same time (Figure S2C). Besides, RIP assay also exhibited that SRSF1 antibody resulted in circ_0007432 and KLF12 enrichment in H1975 and A549 cells (Figures 3J and 3K). It's worth noting that KLF12 enrichment by SRSF1 antibody was decreased by circ_0007432 silencing in NSCLC cells (Figure 3L). As shown in Figures 3M and 3O, SRSF1 was prominently decreased in NSCLC cells transfected with sh-SRSF1. Similar with circ_0007432 knockdown affecting KLF12 expression and the mRNA stability of KLF12, SRSF1 knockdown also resulted in reduced KLF12 expression and weakened KLF12 mRNA stability (Figures 3N–3P). In total, the aforementioned results proved that circ_0007432 elevated KLF12 expression and enhanced KLF12 mRNA stability through recruiting SRSF1.

Circ_0007432 promoted malignant behaviors of NSCLC cells by up-regulating KLF12

Next, we explored whether circ_0007432 affects NSCLC process by regulating KLF12. Firstly, NSCLC cells were transfected with oe-KLF12. KLF12 expression was markedly enhanced in oe-KLF12-transfected H1975 and A549 cells (Figures 4A and 4B). Then circ_0007432-silenced

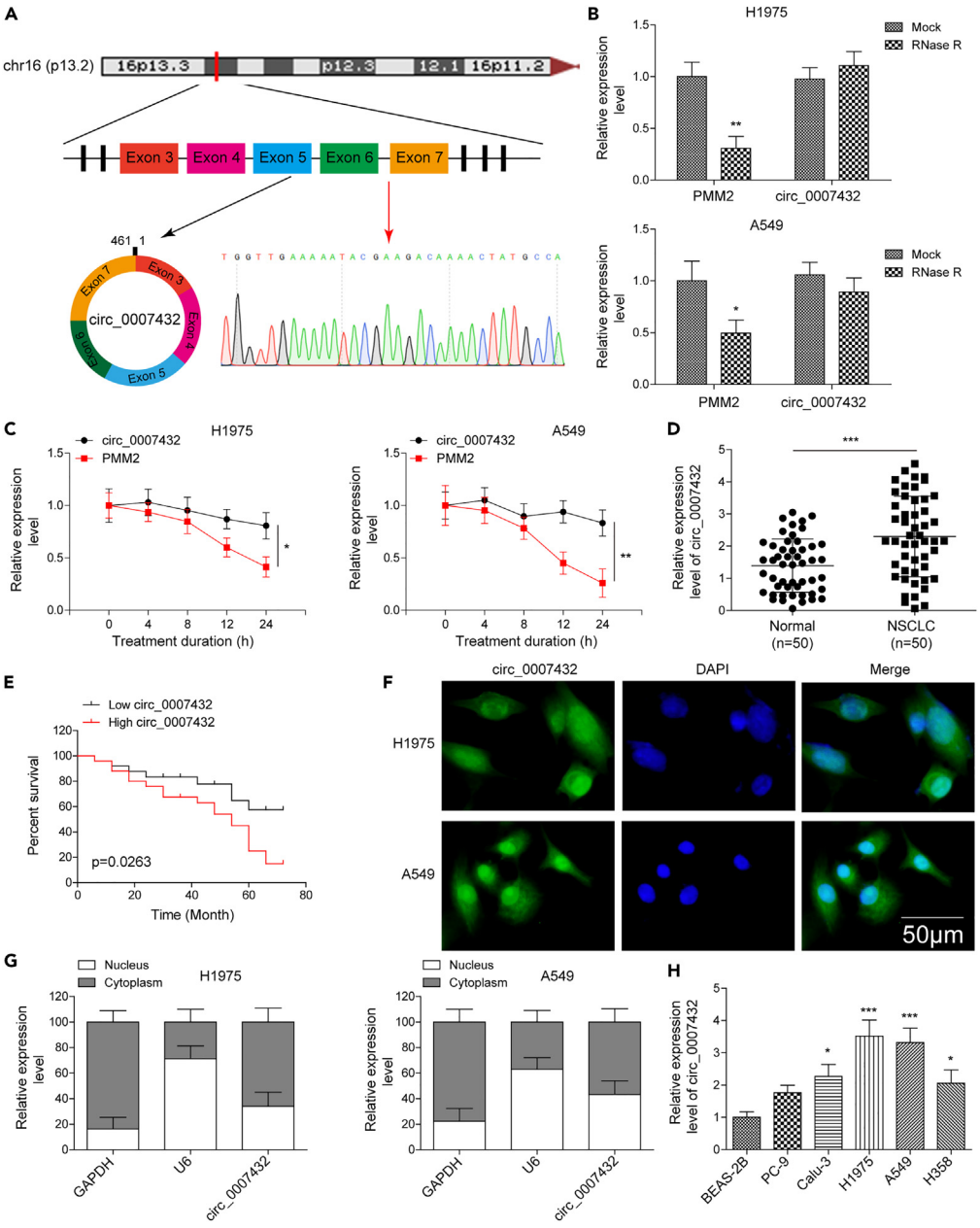

Figure 1. High circ_0007432 expression was observed in NSCLC tissues and cells

(A) Genomic locus of circ_0007432 was determined by Sanger sequencing.

(B and C) RT-qPCR was performed to measure PMM2 and circ_0007432 levels in NSCLC cells upon RNase R treatment or actinomycin D treatment. $n = 3$.

(D) Circ_0007432 expression was detected in tumor tissues and paracancer tissues from NSCLC patients using RT-qPCR. $n = 50$.

(E) The relationship between circ_0007432 and prognosis of NSCLC patients was analyzed using Kaplan-Meier analysis. $n = 50$.

(F and G) Circ_0007432 location in NSCLC cells was determined using FISH and nucleoplasmic separation. $n = 3$. Scale bar: 50 μm.

(H) Circ_0007432 expression was measured in NSCLC cells (PC-9, Calu-3, H1975, A549, and H358) and human bronchial epithelial cells (BEAS-2B) using RT-qPCR. $n = 3$. Data were shown as mean ± SD. Each experiment was accomplished in triplicates. $^{*}p < 0.05$, $^{**}p < 0.01$, $^{***}p < 0.001$. Student's t test for (B), (C), (D), and (H). Kaplan-Meier analysis for (E).

NSCLC cells were transfected with oe-KLF12. As shown in Figures 4C and 4D, circ_0007432 knockdown-mediated suppression of KLF12 expression was reversed by KLF12 overexpression. Furthermore, circ_0007432 silencing-induced inhibition of cell viability and promotion of cell apoptosis as well as changes of Bax and Bcl-2 were abolished by KLF12 overexpression (Figures 4E–4G). Meanwhile, KLF12 overexpression accelerated cell migration and invasion, which impaired circ_0007432 silencing-mediated influences (Figures 4H and 4I).

Table 1. Correlation between circ_0007432 expression and clinical characteristics in non-small cell lung cancer patients

Characteristics	Number (n)	circ_0007432 expression		*p* value
		High	Low	
Age				0.5835
<60	24	10	14	
≥60	26	13	13	
Sex				0.7733
Female	20	11	9	
Male	30	14	16	
Pathological Type				0.6915
Squamous	10	4	6	
Adenocarcinoma	24	13	11	
Large Cell Lung cancer	16	9	7	
T stage				0.0448**
T1 + T2	23	9	14	
T3 + T4	27	19	8	
N stage				0.8233
N0	13	6	7	
N1	23	13	10	
N2	14	7	7	
Grade				0.5094
G1	14	6	8	
G2	17	9	8	
G3	19	12	7	
TNM stage				0.0046**
I + II	28	10	18	
III + IV	22	17	5	
Recurrence or metastasis				0.0450*
No	28	10	18	
Yes	22	15	7	

TNM Staging is referring to the 8th AJCC TNM Staging Criteria. *$p < 0.05$ and **$p < 0.01$.
G1 = well differentiated, G2 = moderately differentiated, G3 = poorly differentiated.

Meanwhile, we also transfected oe-circ_0007432 or together with sh-KLF12 into H1975 and A549 cells. As presented in Figures S3A–S3C, circ_0007432 expression was greatly enhanced by oe-circ_0007432 transfection and KLF12 expression was evidently reduced by sh-KLF12 transfection. Besides, circ_0007432 overexpression resulted in increased KLF12 expression, which was reversed by KLF12 knockdown (Figures S3D and S3E). As expected, circ_0007432 overexpression promoted cell viability and inhibited cell apoptosis, which accompanied by decreasing Bax expression and increasing Bcl-2 expression; however, KLF12 silencing abolished circ_0007432 overexpression-mediated these influences (Figures S3F–S3H). Figures S3I and S3J exhibited that circ_0007432 overexpression promoted cell migration and invasion of NSCLC cells, which were offset by KLF12 silencing. In total, circ_0007432 facilitated the development of NSCLC via modulating KLF12 expression.

KLF12 interacted with IL-8 promoter to transcriptionally activate IL-8

Then, we detected IL-8 expression in tumor tissues by collecting clinical samples. Figure 5A revealed that IL-8 expression was apparently enhanced in tumor tissues compared with para-carcinoma tissues ($n = 50$). Pearson correlation analysis described the positive relationship between IL-8 and KLF12 expression (Figure 5B). Besides, as presented in Figure 5C, we found abnormally higher expression of IL-8 in NSCLC cells including PC-9, Calu-3, H1975, A549, and H358 cells than that in BEAS-2B cells. Moreover, ELISA assay result displayed that the concentration of IL-8 in cellular supernatant of NSCLC cells was high (Figure 5D). These results indicated that IL-8 probably plays a crucial role in NSCLC. JASPAR database predicted the presence of a binding site of KLF12 and IL-8 promoter (Figure 5E). ChIP assay further validated the interaction between KLF12 and IL-8 promoter, evidenced by KLF12 antibody successfully enriching IL-8 promoter (Figure 5F). In addition,

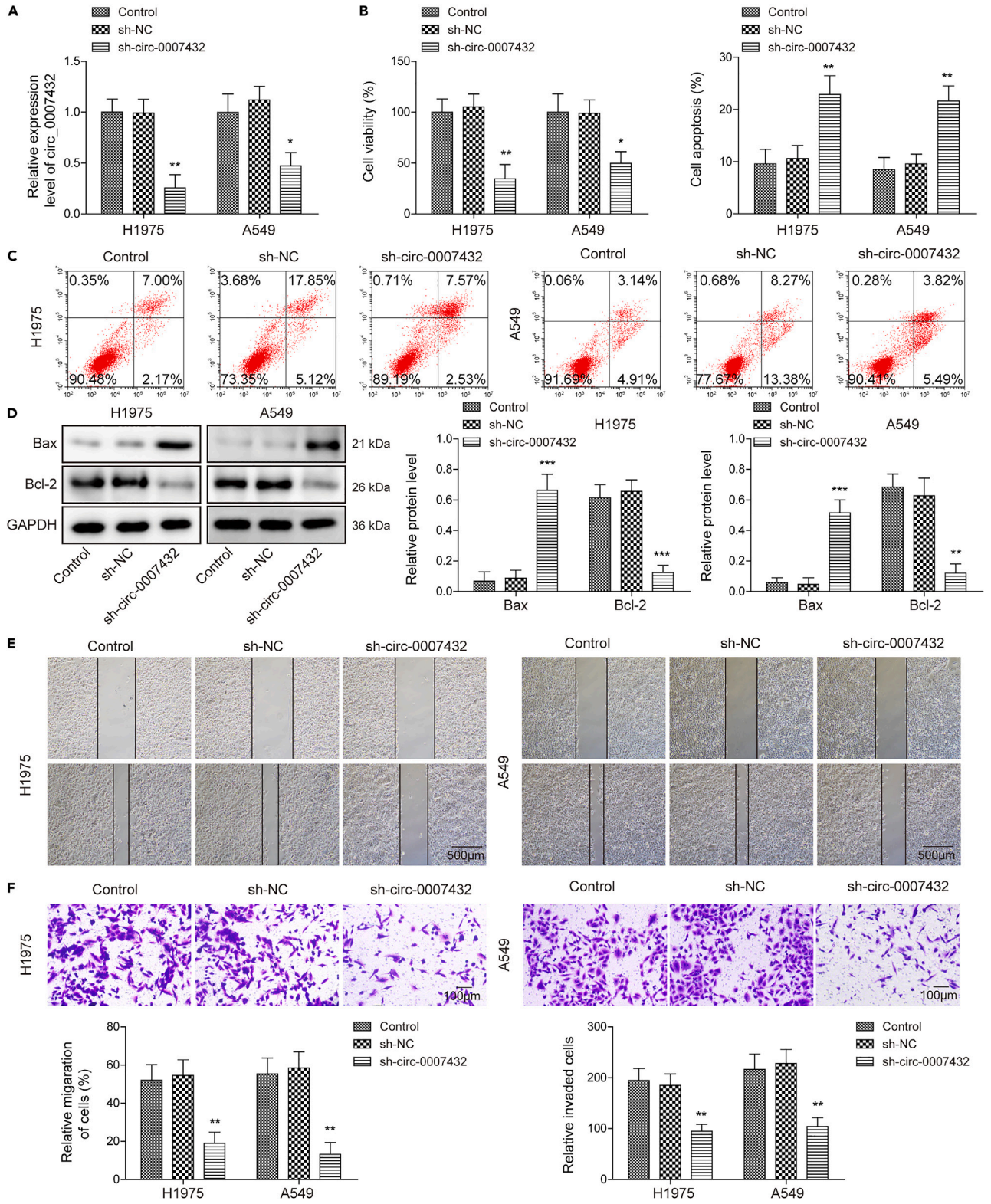

Figure 2. Circ_0007432 silencing suppressed malignant phenotypes of NSCLC sh-NC or sh-circ_0007432 was transfected into H1975 and A549 cells

(A) Circ_0007432 expression was determined using RT-qPCR.

(B) Cell viability was evaluated by CCK-8.

Figure 2. *Continued*

(C) Cell apoptosis was examined using flow cytometry.

(D) Bax and Bcl-2 levels were measured using western blot.

(E and F) Cell migration (scale bar: 500 μm) and invasion (scale bar: 100 μm) were evaluated by wound healing and transwell assay. $n = 3$. Data were shown as mean ± SD. Each experiment was accomplished in triplicates. *$p < 0.05$, **$p < 0.01$, ***$p < 0.001$. One-way analysis of variance (ANOVA) was performed.

luciferase activity in WT-IL-8 group was apparently attenuated by sh-KLF12, while had no impacts in MUT-IL-8 group (Figure 5G). Further experiments found that KLF12 downregulation led to decreased IL-8 mRNA expression and secretion in H1975 and A549 cells (Figures 5H and 5I). All in all, IL-8 expression and secretion are enhanced in NSCLC cells and KLF12 promoted IL-8 levels through interacting with IL-8 promoter.

Circ_0007432 promoted M2 macrophage polarization by upregulating KLF12 and IL-8 levels

To explore the role of circ_0007432/KLF12/IL-8 axis in macrophage polarization, THP-1 cells were co-incubated with NSCLC cells that underwent sh-circ_0007432 or along with oe-KLF12 transfections. The cell co-culture model diagram was presented in Figure 6A. Subsequently, we detected the protein level of IL-8 in THP-1 cells. Circ_0007432 knockdown resulted in decreased IL-8 level in THP-1 cells, whereas KLF12 upregulation rescued the effects of circ_0007432 knockdown (Figure 6B). As anticipated, circ_0007432 knockdown could enhance the expression of M1 macrophage markers (IL-6, TNF-α, and IL-1β) and decrease the expression of M2 macrophage markers (IL-10, CCL22, and Arg-1). However, circ_0007432 knockdown-mediated these alterations were abolished by KLF12 upregulation (Figure 6C). Furthermore, CD86 (an M1 macrophage marker) and CD206 (an M2 macrophage marker) positive cells were examined by flow cytometry. We found that circ_0007432 silencing induced more CD86 positive cells while reduced CD206 positive cells, these phenomena were reversed by KLF12 overexpression (Figure 6D). To provide more evidence supporting influences of circ_0007432/KLF12/IL-8 axis on M2 macrophage polarization, THP-1 cells were co-incubated with NSCLC cells that were treated with oe-circ_0007432 or along with sh-KLF12 transfection or addition of IL-8 antibody. We found that circ_0007432 overexpression could upregulate IL-8 protein levels in macrophages, KLF12 knockdown or IL-8 antibody reversed circ_0007432 overexpression-mediated upregulation of IL-8 expression (Figure S4A). Circ_0007432 upregulation decreased the expressions of IL-6, TNF-α, and IL-1β and elevated the expressions of IL-10, CCL22, and Arg-1, whereas KLF12 knockdown or IL-8 antibody reversed these alterations caused by circ_0007432 overexpression (Figure S4B). Flow cytometry exhibited circ_0007432 overexpression resulted in decreased CD86 positive cells and increased CD206 positive cells, which were compromised by KLF12 knockdown or IL-8 antibody (Figure S4C). Taken together, circ_0007432 in NSCLC cells promoted the polarization of macrophages to M2 type by increasing KLF12 and IL-8.

Circ_0007432 promoted tumorigenesis in mice and M2 macrophage polarization by affecting KLF12

Finally, *in vivo* experiments were conducted to further validate the role of circ_0007432 in NSCLC and macrophage polarization. sh-circ_0007432 or oe-KLF12 were stably transfected into A549 cells. Transfected A549 cells were injected subcutaneously into mice. After 25 days, tumor tissue was collected for follow-up experiments. As a result, circ_0007432 silencing suppressed tumor sizes and weights, while KLF12 overexpression could attenuate influences of circ_0007432 silencing on tumor sizes and weights (Figures 7A–7C). Besides, circ_0007432 and KLF12 expression was declined by circ_0007432 silencing, which was compromised by KLF12 upregulation (Figures 7D and 7E). Lower level of Ki67 (a marker of cell proliferation) was observed in sh-circ_0007432 group. However, Ki67 level was enhanced in sh-circ_0007432+ oe-KLF12 group (Figure 7F). As expected, circ_0007432 knockdown reduced IL-8 expression, whereas KLF12 overexpression reversed circ_0007432 knockdown-mediated reduction of IL-8 expression (Figure 7G). As shown in Figure 7H, circ_0007432 knockdown elevated IL-6, TNF-α, and IL-1β expressions and reduced IL-10, CCL22, and Arg-1 expressions, which were compromised by KLF12 overexpression. In conclusion, circ_0007432 knockdown suppressed *in vivo* tumorigenesis and M2 macrophage polarization of NSCLC by downregulating KLF12 expression.

DISCUSSION

Due to high incidence and high mortality of NSCLC, numerous patients have lost their precious lives. Substantial evidence has determined that inhibiting malignant behaviors of NSCLC cells and suppressing M2 macrophage polarization in TME have identified as effective research approaches for cancer treatments.[26,27] In this study, we found that circ_0007432 knockdown inhibited SRSF1/KLF12/IL-8 axis to suppress viability, migration and invasion of NSCLC cells and M2 macrophage polarization, thereby delaying NSCLC progression, which might provide promising intervention targets for NSCLC treatment.

In recent years, circRNA has received increasing attention for its role in disease, particularly in oncology field.[28] Although the vast majority of circRNAs cannot encode proteins, they could perform various functions, such as sponge adsorption of miRNAs, regulation of transcription initiation and elongation, recruitment of epigenetic modification factors, and regulation of differential splicing.[12,29,30] In some cases, circRNAs also encode small peptides.[31] Numerous circRNAs was reported to play vital roles in NSCLC progression. For instance, circRNA OXCT1 and circRHOT1 were reported to accelerate NSCLC progression.[14,32] In addition, circRNAs were closely related with M2 macrophage polarization in TME. As previously documented, extracellular vesicle-carrying circATP2B4 promoted M2 macrophage polarization through miR-532-3p/SREBF1 axis to facilitate epithelial ovarian cancer.[33] In NSCLC, exosomes carrying circSHKBP1 that derived from NSCLC cells promoted M2 macrophage polarization and macrophage recruitment via elevating PKM2

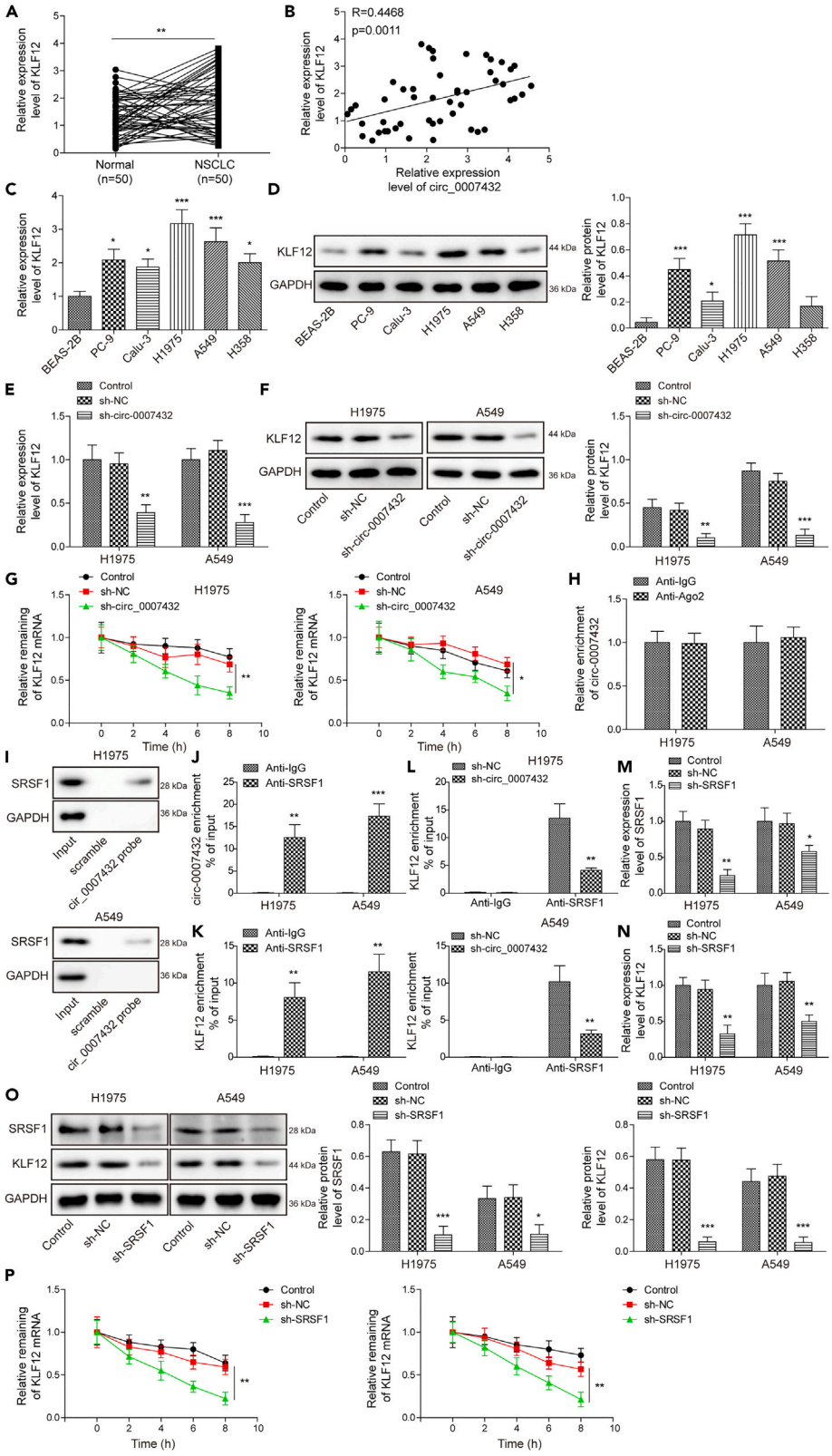
A
Relative expression level of KLF12
Normal (n=50)
NSCLC (n=50)
B
R=0.4468
p=0.0011
Relative expression level of KLF12
Relative expression level of circ_0007432
C
Relative expression level of KLF12
BEAS-2B
PC-9
Calu-3
H1975
A549
H358
D
KLF12
GAPDH
44 kDa
36 kDa
Relative protein level of KLF12
E
Control
sh-NC
sh-circ-0007432
Relative expression level of KLF12
F
H1975
A549
Relative protein level of KLF12
G
sh-circ_0007432
Relative remaining of KLF12 mRNA
Time (h)
H
Anti-IgG
Anti-Ago2
Relative enrichment of circ-0007432
I
SRSF1
28 kDa
Input
scramble
circ_0007432 probe
J
Anti-SRSF1
circ-0007432 enrichment % of input
K
KLF12 enrichment % of input
L
M
Relative expression level of SRSF1
N
Relative expression level of KLF12
O
sh-SRSF1
Relative protein level of SRSF1
P

Figure 3. Circ_0007432 maintained KLF12 mRNA stability by recruiting SRSF1

(A) KLF12 expression was detected in tumor tissues and corresponding adjacent tissues from NSCLC patients using RT-qPCR. $n = 50$.

(B) The relationship between circ_0007432 and KLF12 in NSCLC was analyzed using Pearson correlation analysis. $n = 50$.

(C and D) KLF12 expression was measured in NSCLC cells (PC-9, Calu-3, H1975, A549, and H358) and BEAS-2B cells using RT-qPCR and western blot. $n = 3$.

(E and F) KLF12 expression was evaluated in sh-NC- or sh-circ_0007432-transfected H1975 and A549 cells by RT-qPCR and western blot. $n = 3$.

(G) The stability of KLF12 mRNA was detected in sh-NC- or sh-circ_0007432-transfected NSCLC cells by RT-qPCR. $n = 3$.

(H) The interaction between circ_0007432 and Ago2 in NSCLC cells were evaluated using RIP. $n = 3$.

(I and J) The interaction between circ_0007432 and SRSF1 was validated using RNA pull down and RIP. $n = 3$.

(K and L) The interaction between KLF12 and SRSF1 was validated using RIP. $n = 3$.

(M–O) SRSF1 and KLF12 expression was detected in sh-NC- or sh-SRSF1-transfected H1975 and A549 cells by RT-qPCR and western blot. $n = 3$.

(P) The stability of KLF12 mRNA was detected in sh-NC- or sh-SRSF1-transfected NSCLC cells by RT-qPCR. $n = 3$. Data were shown as mean ± SD. Each experiment was accomplished in triplicates. $^{*}p < 0.05$, $^{**}p < 0.01$, $^{***}p < 0.001$. Student's t test for (A), (C), (D), (H), (J), (K), and (L). Pearson correlation analysis for (B). One-way analysis of variance (ANOVA) test for (E), (F), (G), (M), (N), (O), and (P).

expression.[34] Some circRNAs that played crucial roles in NSCLC were expected to be promising biomarkers or therapeutic targets for the diagnosis of NSCLC.[35] For instance, Shaoyan Zhang et al. indicated that circ_0014130 was recommended as a predictive biomarker in NSCLC.[36] Encouragingly, a previous study pointed out that circ_0007432 was abnormally high expressed in tumor tissues of NSCLC patients by human circRNAs chip screening.[17] Currently, the role of circ_0007432 in tumors and its molecular regulation mechanism are still blank. Our findings revealed that higher expression of circ_0007432 was observed in tumor tissues from NSCLC patients and contributed to poor prognosis. Further experiments validated that circ_0007432 inhibition suppressed the progression of NSCLC through restraining malignant behaviors in cells and mice. Our findings revealed the promoting effects of circ_0007432 on cell growth and M2 macrophage polarization in NSCLC.

KLF12 was identified as an oncogene in various tumor researches. For instance, KLF12 was regulated by lncRNA DANCR/miR-216a-5p axis to accelerate hepatocellular carcinoma malignancy.[37] LINC00319 upregulated KLF12 expression through sponging miR-1207-5p to promote nasopharyngeal carcinoma carcinogenesis.[38] Circ-RNF111 targeted miR-876-3p to increase KLF12 expression, which accelerated malignancy of gastric cancer.[39] These studies suggested that KLF12 played promoting roles in tumors. In our study, abnormally higher expression of KLF12 was observed in tissues from NSCLC patients, which was consistent with a published study.[20] Moreover, circ_0007432 expression was positively related with KLF12 expression in NSCLC tissues, and circ_0007432 promoted malignant behaviors of NSCLC cells by up-regulating KLF12 expression.

At present, accumulating studies put forward that circRNAs could affect gene expression through interacting with RNA-binding protein.[40] For instance, circDNAJC11 interacted with TAF15 (an RBP) to stabilize MAPK6 mRNA and enhance MAPK6 expression, thereby accelerating cell growth of breast cancer.[41] Here, we confirmed that circ_0007432 could stabilize KLF12 mRNA through binding to SRSF1 in NSCLC. SRSF1 belongs to the conserved SR protein family, which includes 12 members and plays important roles in multiple diseases through multifaceted regulators of gene expression.[42] It has been reported that SRSF1 can be used as RBP to regulate gene expression. For example, SRSF1 acted as an RBP interacting with circ_0001052 to stabilize Hipk3 mRNA in cardiac hypertrophy.[43] Furthermore, we demonstrated that KLF12 overexpression abolished circ_0007432 silencing-mediated anti-malignant behaviors of NSCLC cells. In this study, we determined that circ_0007432 stabilized and elevated KLF12 mRNA stability to promote cell growth of NSCLC cells through recruiting SRSF1. Our study unlocks the important role of circ_000743 in NSCLC and its regulatory mechanism, which lays an important theoretical foundation for future drug research using circ_000743 as a molecular target. Antisense oligonucleotide (ASO) therapy, which targets RNAs, is a class of molecular drugs that inhibit the expression of the target genes by sequence-specific binding to the target gene DNA or mRNA to regulate genes' expression. Antisense oligonucleotides provide a way to regulate target genes involved in cancer progression. ASO is not only a useful experimental tool for protein target identification and validation, but also a highly selective therapeutic strategy for diseases with dysregulated protein expression.[44] Chemical modification of antisense oligonucleotides increases resistance to nuclease digestion, prolongs tissue half-life, and improves scheduling.[45] It will be of great clinical significance to further develop antisense oligonucleotide therapy targeting circ_0007432 to further verify its efficacy in NSCLC.

It is well-known that IL-8, a leukocyte chemical attractant, is closely related with immune response.[46] In recent years, growing evidence has demonstrated IL-8 level was elevated in tumor cells, infiltrating neutrophils, endothelial cells, and TAM, suggesting IL-8 is a crucial factor in TME. Furthermore, there were some substantial evidences found that IL-8 was relevant to M2 macrophage polarization and cancer progression.[47] As previously studied, CD163 and CD206 expression was observably elevated in THP-1 cells that were co-cultured with bladder cancer cells or following the addition of exogenous IL-8, suggesting IL-8 was equipped to promote M2 macrophage polarization.[48] Here, IL-8 expression and secretion was elevated by KLF12 through interacting with IL-8 promoter. In addition, circ_0007432 silencing suppressed IL-8 expression and secretion, which was reversed by KLF12 overexpression. Based on the effects of IL-8 on macrophage polarization, in this study, circ_0007432 facilitated KLF12 to upregulate IL-8 in NSCLC cells, thus promoting M2 macrophage polarization both *in vitro* and *in vivo*. It is well-accepted that macrophages are important components of TME, which closely influences on tumor progression.[49] Growing evidences have demonstrated that M2 macrophage polarization contributed to development of tumors.[50] Here, we merely detected the role of circ_0007432 in promoting M2 macrophage polarization by influencing IL-8 secretion. Whether activated macrophages induced by circ_0007432 further aggravate the tumor progression is worthy of further exploration. Moreover, whether circ_0007432 exists in macrophages and other immune cells in the TME, and how the abnormal expression of circ_0007432 in these cells affects the TME can be another interesting topic to explore in the future.

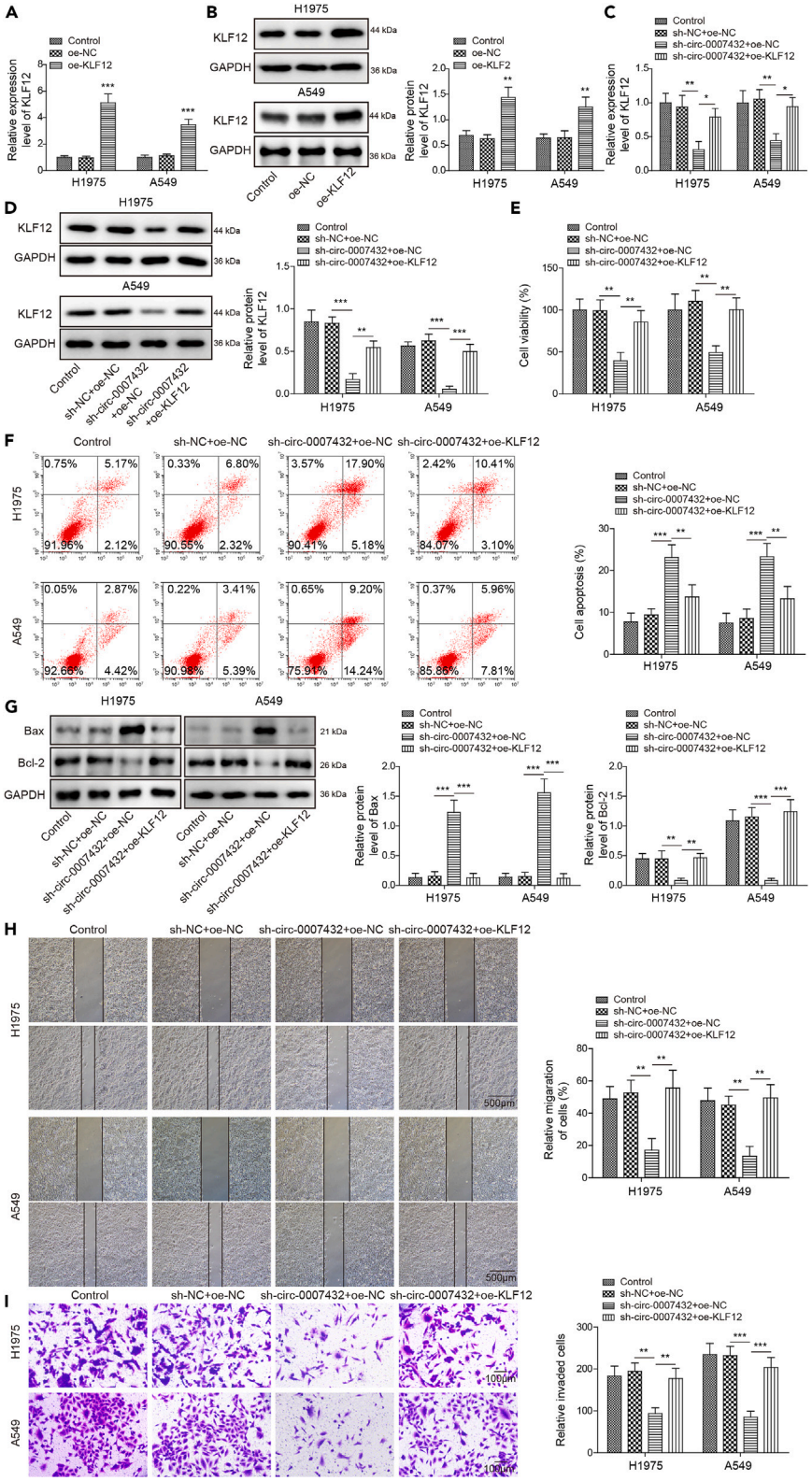
A
Control
oe-NC
oe-KLF12
Relative expression level of KLF12
H1975
A549
B
H1975
KLF12
GAPDH
44 kDa
36 kDa
A549
Control
oe-NC
oe-KLF12
Relative protein level of KLF12
oe-KLF2
C
Control
sh-NC+oe-NC
sh-circ-0007432+oe-NC
sh-circ-0007432+oe-KLF12
Relative expression level of KLF12
D
H1975
KLF12
GAPDH
A549
Control
sh-NC+oe-NC
sh-circ-0007432 +oe-NC
sh-circ-0007432 +oe-KLF12
Relative protein level of KLF12
E
Cell viability (%)
F
Control
sh-NC+oe-NC
sh-circ-0007432+oe-NC
sh-circ-0007432+oe-KLF12
H1975
A549
0.75%
5.17%
91.96%
2.12%
0.33%
6.80%
90.55%
2.32%
3.57%
17.90%
90.41%
5.18%
2.42%
10.41%
84.07%
3.10%
0.05%
2.87%
92.66%
4.42%
0.22%
3.41%
90.98%
5.39%
0.65%
9.20%
75.91%
14.24%
0.37%
5.96%
85.86%
7.81%
Cell apoptosis (%)
G
H1975
A549
Bax
Bcl-2
GAPDH
21 kDa
26 kDa
36 kDa
Control
sh-NC+oe-NC
sh-circ-0007432+oe-NC
sh-circ-0007432+oe-KLF12
Relative protein level of Bax
Relative protein level of Bcl-2
H
Control
sh-NC+oe-NC
sh-circ-0007432+oe-NC
sh-circ-0007432+oe-KLF12
H1975
A549
500μm
Relative migaration of cells (%)
I
Control
sh-NC+oe-NC
sh-circ-0007432+oe-NC
sh-circ-0007432+oe-KLF12
H1975
A549
100μm
Relative invaded cells

Figure 4. Circ_0007432 promoted malignant behaviors of NSCLC cells by up-regulating KLF12

(A and B) The overexpression efficiency of oe-KLF12 was validated using RT-qPCR and western blot. Oe-NC or oe-KLF12 was transfected into circ_0007432-silenced NSCLC cells.

(C and D) KLF12 expression was detected by RT-qPCR and western blot.

(E) Cell viability was evaluated by CCK-8.

(F) Cell apoptosis was examined using flow cytometry.

(G) Bax and Bcl-2 levels were measured using western blot.

(H and I) Cell migration (scale bar: 500 μm) and invasion (scale bar: 100 μm) were evaluated by wound healing and transwell. $n = 3$. Data were shown as mean ± SD. Each experiment was accomplished in triplicates. $^{*}p < 0.05$, $^{**}p < 0.01$, $^{***}p < 0.001$. One-way analysis of variance (ANOVA) was performed.

In conclusion, circ_0007432 enhanced KLF12-mediated elevation of IL-8 expression and secretion in NSCLC cells through recruiting SRSF1, thereby promoting NSCLC progression and M2 macrophage polarization. Our study sheds light on the mechanism of IL-8 release in malignant behavior of NSCLC cells, providing a potential therapeutic target for the treatment of NSCLC.

Limitations of the study

Of course, there are many limitations to our study: the mechanism exploration in this study was mainly based on *in vitro* cell line experiments, and have limitations in terms of the complexity of tumor biology *in vivo*; other potential functions and mechanisms of circ_0007432 beyond the SRSF1/KLF12 axis need to be further explored; the downstream signaling and functional effects of IL-8 on macrophages have not been fully explored; whether the findings apply to other cancer types or clinical situations remains to be determined; the clinical relevance of the findings was based on a relatively small sample of NSCLC tissues. Larger and more diverse patient cohorts would strengthen the conclusions; our study focused on a limited number of NSCLC cell lines and did not take into account tumor/cell line heterogeneity; the effects of circ_0007432 knockdown on the expression of other factors were not detected by sequencing and proteomic analysis. Whether circ_0007432 knockdown affects other factors and whether this effect could further regulate other immune cells and thus regulate the tumorigenesis and development are worthy of further exploration; the single-cell method can better characterize the state of macrophages; in addition, the application of genetically engineered mouse models can better study tumor immune interactions under carrier conditions. However, these experiments were not carried out in this study. We look forward to completing each of these in near future to further confirm the important value of circ_0007432 in tumor prediction, treatment, and TME.

STAR★METHODS

Detailed methods are provided in the online version of this paper and include the following:

- KEY RESOURCES TABLE
- RESOURCE AVAILABILITY
  - Lead contact
  - Materials availability
  - Data and code availability
- EXPERIMENTAL MODEL AND STUDY PARTICIPANT DETAILS
- METHOD DETAILS
  - Co-culture system of THP-1 cells and NSCLC cells
  - Cell transfection
  - RNase R digestion
  - RNA stability
  - RT-qPCR
  - Fluorescence *in situ* hybridization (FISH)
  - Nuclear/cytoplasmic fractionation
  - Cell counting kit-8 (CCK-8) assay
  - Flow cytometry
  - Western blot
  - Wound healing assay
  - Transwell assay
  - RNA-binding protein immunoprecipitation (RIP)
  - RNA pull-down assay
  - RNA electrophoretic mobility shift assay (EMSA)
  - Enzyme-linked immunosorbent assay (ELISA)
  - Chromatin immunoprecipitation (ChIP) assay
  - Dual luciferase reporter assay
  - Tumor formation in nude mice

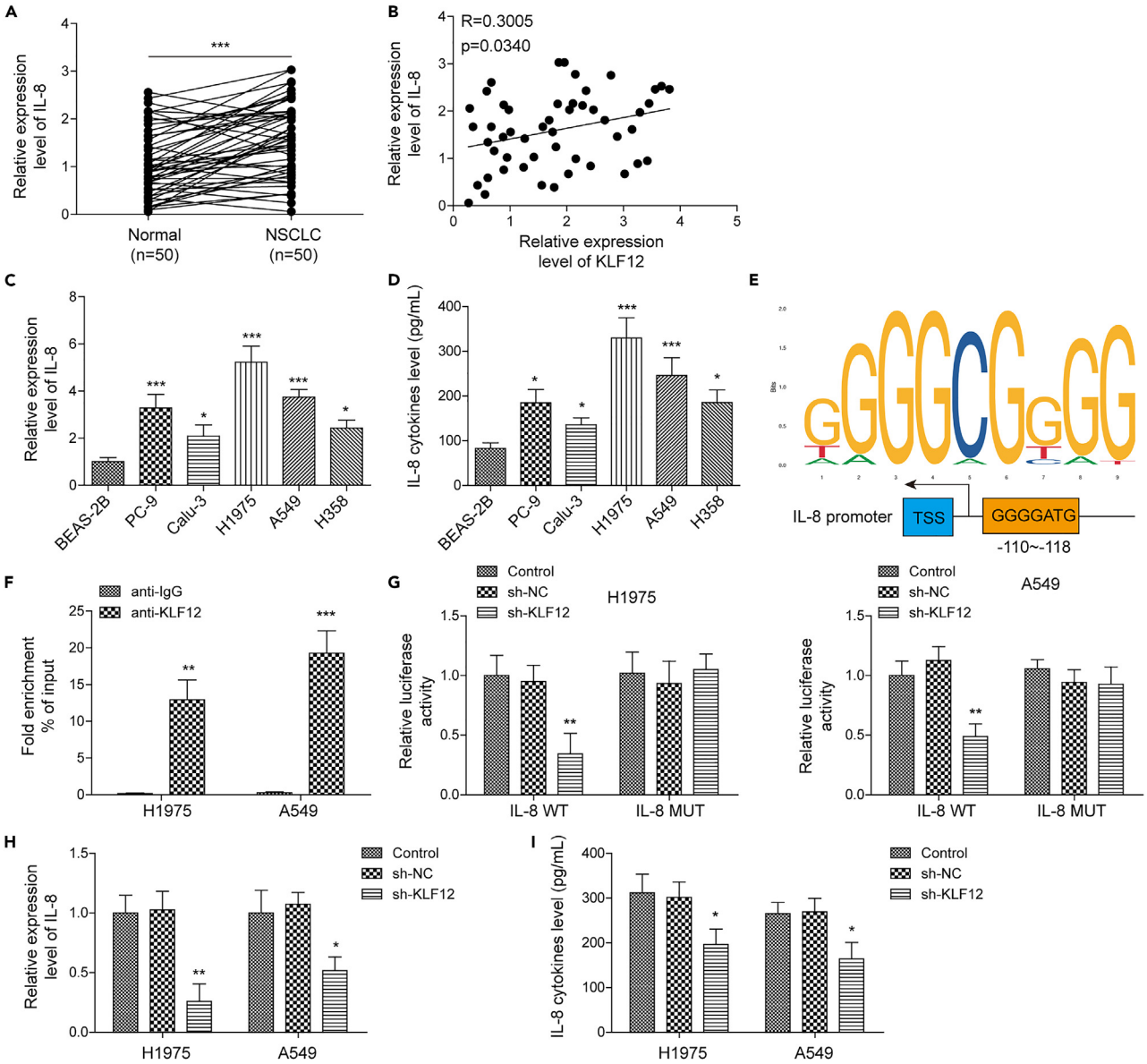

Figure 5. KLF12 interacted with IL-8 promoter to transcriptionally activate IL-8

(A) IL-8 expression was detected in tumor tissues and corresponding adjacent tissues from NSCLC patients using RT-qPCR. $n = 50$.

(B) The relationship between IL-8 and KLF12 in NSCLC was analyzed using Pearson correlation analysis. $n = 50$.

(C and D) IL-8 expression and IL-8 secretion were measured in NSCLC cells (PC-9, Calu-3, H1975, A549, and H358) and BEAS-2B cells using RT-qPCR and ELISA. $n = 3$.

(E) The binding site between KLF12 and IL-8 promoter was predicted using JASPAR database. $n = 3$.

(F and G) The interaction between KLF12 and IL-8 promoter was validated by ChIP and dual luciferase assay. $n = 3$.

(H and I) IL-8 expression and IL-8 secretion were measured in sh-NC- or sh-KLF12-transfected H1975 and A549 cells using RT-qPCR and ELISA. $n = 3$. Data were shown as mean ± SD. Each experiment was accomplished in triplicates. $^*p < 0.05$, $^{**}p < 0.01$, $^{***}p < 0.001$. Student's t test for (A), (C), (D), and (F). Pearson correlation analysis for (B). One-way analysis of variance (ANOVA) for (G), (H), and (I).

- ○ Immunohistochemical (IHC) staining
- ● QUANTIFICATION AND STATISTICAL ANALYSIS

SUPPLEMENTAL INFORMATION

Supplemental information can be found online at https://doi.org/10.1016/j.isci.2024.109861.

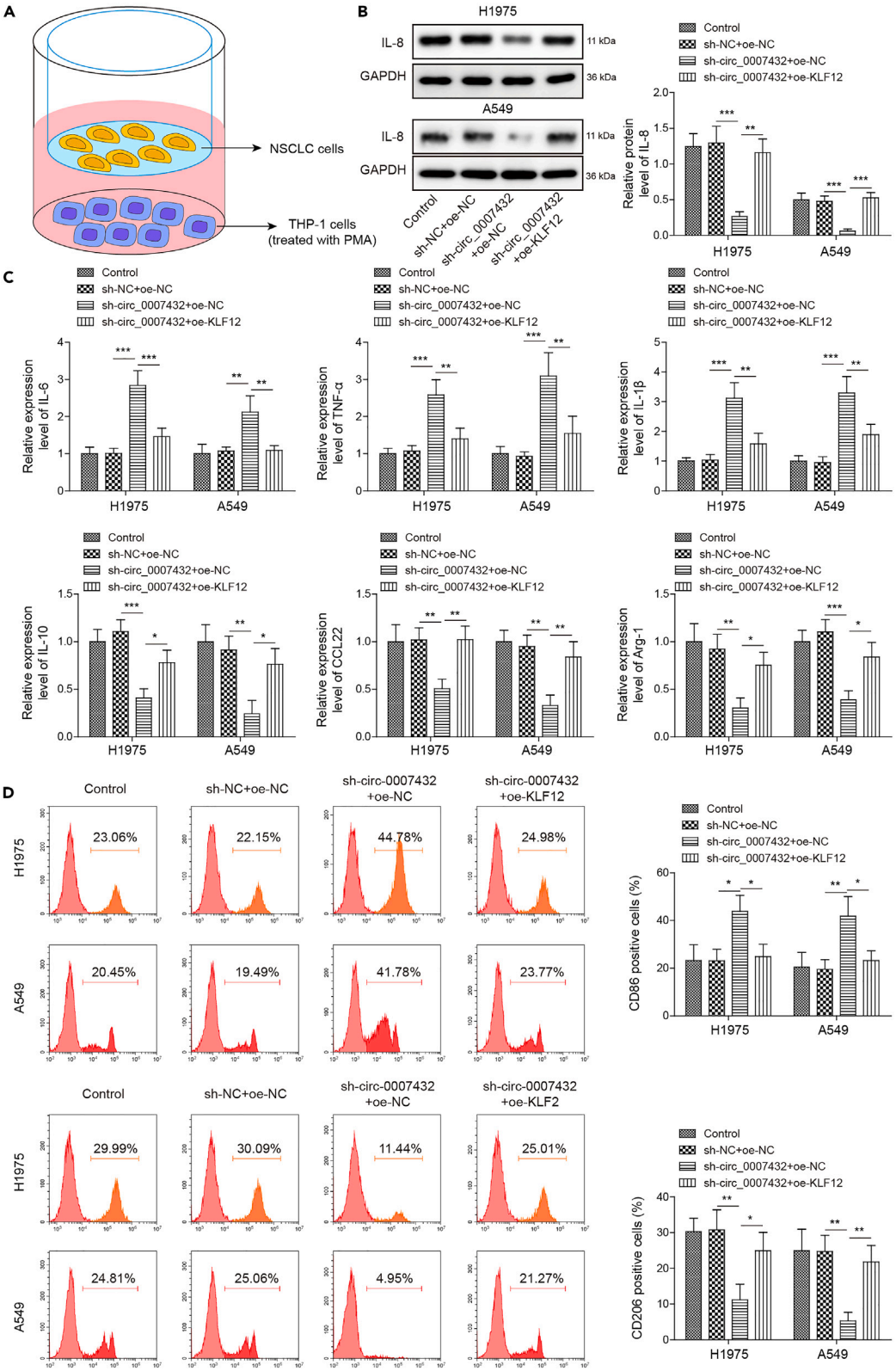
A
NSCLC cells
THP-1 cells
(treated with PMA)
B
H1975
IL-8
GAPDH
11 kDa
36 kDa
A549
Control
sh-NC+oe-NC
sh-circ_0007432 +oe-NC
sh-circ_0007432 +oe-KLF12
Relative protein level of IL-8
C
Relative expression level of IL-6
Relative expression level of TNF-α
Relative expression level of IL-1β
Relative expression level of IL-10
Relative expression level of CCL22
Relative expression level of Arg-1
H1975
A549
D
Control
sh-NC+oe-NC
sh-circ-0007432 +oe-NC
sh-circ-0007432 +oe-KLF12
23.06%
22.15%
44.78%
24.98%
20.45%
19.49%
41.78%
23.77%
CD86 positive cells (%)
sh-circ-0007432 +oe-KLF2
29.99%
30.09%
11.44%
25.01%
24.81%
25.06%
4.95%
21.27%
CD206 positive cells (%)

Figure 6. Circ_0007432 promoted M2 macrophage polarization by upregulating KLF12 and IL-8 levels

(A) The co-culture model diagram of THP-1 cells and NSCLC cells. THP-1 cells treated with PAM were co-incubated with H1975 (Co-H1975) or A549 (Co-A549) cells that were transfected with sh-circ_0007432 or along with oe-KLF12.

(B) IL-8 protein levels in THP-1 cells were detected using western blot. $n = 3$.

(C) IL-6, TNF-α, IL-1β, IL-10, CCL22, and Arg-1 levels in THP-1 cells were detected by RT-qPCR. $n = 3$.

(D) CD86 or CD206 positive cells in THP-1 cells were evaluated using flow cytometry. $n = 3$. Data were shown as mean ± SD. Each experiment was accomplished in triplicates. $^{*}p < 0.05$, $^{**}p < 0.01$, $^{***}p < 0.001$. One-way analysis of variance (ANOVA) for (B), (C), and (D).

ACKNOWLEDGMENTS

This work was supported by Hainan Provincial Natural Science Foundation of China (822RC862) and Hainan Province Clinical Medic cal Center No.(2021)75 and No.(2021)276.

AUTHOR CONTRIBUTIONS

S.M. and J.W. designed this study. S.M., D.W., and X.C. collected the materials and performed the experiments. S.M. analyzed the data and wrote the manuscript. J.W. revised the manuscript. All authors read and approved the final version of the manuscript.

DECLARATION OF INTERESTS

These authors declared no competing interests in this work.

Received: November 8, 2023
Revised: March 5, 2024
Accepted: April 27, 2024
Published: April 30, 2024

REFERENCES

1. Sung, H., Ferlay, J., Siegel, R.L., Laversanne, M., Soerjomataram, I., Jemal, A., and Bray, F. (2021). Global cancer statistics 2020: Globocan estimates of incidence and mortality worldwide for 36 cancers in 185 countries. CA. Cancer J. Clin. *71*, 209–249.
2. Osmani, L., Askin, F., Gabrielson, E., and Li, Q.K. (2018). Current who guidelines and the critical role of immunohistochemical markers in the subclassification of non-small cell lung carcinoma (nsclc): Moving from targeted therapy to immunotherapy. Semin. Cancer Biol. *52*, 103–109.
3. Chaft, J.E., Rimner, A., Weder, W., Azzoli, C.G., Kris, M.G., and Cascone, T. (2021). Evolution of systemic therapy for stages i-iii non-metastatic non-small-cell lung cancer. Nat. Rev. Clin. Oncol. *18*, 547–557.
4. Maemondo, M. (2016). Tyrosine kinase inhibitors as first-line treatment in nsclc. Lancet Oncol. *17*, 541–543.
5. Hanahan, D., and Coussens, L.M. (2012). Accessories to the crime: Functions of cells recruited to the tumor microenvironment. Cancer Cell *21*, 309–322.
6. Shu, Y., and Cheng, P. (2020). Targeting tumor-associated macrophages for cancer immunotherapy. Biochim. Biophys. Acta. Rev. Cancer *1874*, 188434.
7. Wang, Y., Smith, W., Hao, D., He, B., and Kong, L. (2019). M1 and m2 macrophage polarization and potentially therapeutic naturally occurring compounds. Int. Immunopharmacol. *70*, 459–466.
8. Fu, L.Q., Du, W.L., Cai, M.H., Yao, J.Y., Zhao, Y.Y., and Mou, X.Z. (2020). The roles of tumor-associated macrophages in tumor angiogenesis and metastasis. Cell. Immunol. *353*, 104119.
9. Lin, Y., Xu, J., and Lan, H. (2019). Tumor-associated macrophages in tumor metastasis: Biological roles and clinical therapeutic applications. J. Hematol. Oncol. *12*, 76.
10. Mao, X., Xu, J., Wang, W., Liang, C., Hua, J., Liu, J., Zhang, B., Meng, Q., Yu, X., and Shi, S. (2021). Crosstalk between cancer-associated fibroblasts and immune cells in the tumor microenvironment: New findings and future perspectives. Mol. Cancer *20*, 131.
11. Li, X., Yang, L., and Chen, L.L. (2018). The biogenesis, functions, and challenges of circular rnas. Mol. Cell *71*, 428–442.
12. Chen, L.L. (2020). The expanding regulatory mechanisms and cellular functions of circular rnas. Nat. Rev. Mol. Cell Biol. *21*, 475–490.
13. Wang, Z.H., Ye, L.L., Xiang, X., Wei, X.S., Niu, Y.R., Peng, W.B., Zhang, S.Y., Zhang, P., Xue, Q.Q., Wang, H.L., et al. (2023). Circular rna circfbxo7 attenuates non-small cell lung cancer tumorigenesis by sponging mir-296-3p to facilitate klf15-mediated transcriptional activation of cdkn1a. Transl. Oncol. *30*, 101635.
14. Luo, H., Peng, J., and Yuan, Y. (2023). Circrna oxct1 promotes the malignant progression and glutamine metabolism of non-small cell lung cancer by absorbing mir-516b-5p and upregulating slc1a5. Cell Cycle *22*, 1182–1195. https://doi.org/10.1080/15384101.2022.2071565:1-14.
15. Yang, W., Yao, Y., Yang, S., and Ke, Y. (2023). Circular rna hsa_circ_0008003 promotes the progression of non-small-cell lung cancer by sponging mir-548i and regulating kpna4 expression. Thorac. Cancer *14*, 544–554.
16. Zhang, Q., Ding, F., Zhang, C., Han, X., and Cheng, H. (2023). Circ_0001715 functions as a mir-1249-3p sponge to accelerate the progression of non-small cell lung cancer via upregulating the level of fgf5. Biochem. Genet. *61*, 1807–1826. https://doi.org/10.1007/s10528-023-10344-6.
17. Jiang, M.M., Mai, Z.T., Wan, S.Z., Chi, Y.M., Zhang, X., Sun, B.H., and Di, Q.G. (2018). Microarray profiles reveal that circular rna hsa_circ_0007385 functions as an oncogene in non-small cell lung cancer tumorigenesis. J. Cancer Res. Clin. Oncol. *144*, 667–674.
18. Guan, B., Li, Q., Zhang, H.Z., and Yang, H.S. (2020). Circ_notch3 functions as a protooncogene competing with mir-205-5p, modulating klf12 expression and promoting the development and progression of basal-like breast carcinoma. Front. Oncol. *10*, 602694.
19. Yang, J., Liu, Z., Liu, B., and Sun, L. (2022). Silencing of circcyp51a1 represses cell progression and glycolysis by regulating mir-490-3p/klf12 axis in osteosarcoma under hypoxia. J. Bone Oncol. *37*, 100455.
20. Liu, Y., Liang, L., Ji, L., Zhang, F., Chen, D., Duan, S., Shen, H., Liang, Y., and Chen, Y. (2021). Potentiated lung adenocarcinoma (luad) cell growth, migration and invasion by lncrna dars-as1 via mir-188-5p/klf12 axis. Aging (Albany NY) *13*, 23376–23392.
21. Lu, X., Han, Y., Han, Y., Huang, M., You, J., Liu, Y., Ding, Y., and Zheng, Y. (2022). Microrna-650 suppresses klf12 expression to regulate growth and metastasis of human ovarian cancer cells. Acta Biochim. Pol. *69*, 745–751.
22. Valeta-Magara, A., Gadi, A., Volta, V., Walters, B., Arju, R., Giashuddin, S., Zhong, H., and Schneider, R.J. (2019). Inflammatory breast cancer promotes development of m2 tumor-associated macrophages and cancer mesenchymal cells through a complex chemokine network. Cancer Res. *79*, 3360–3371.
23. Zhao, Y., Sun, J., Li, Y., Zhou, X., Zhai, W., Wu, Y., Chen, G., Gou, S., Sui, X., Zhao, W., et al. (2021). Tryptophan 2,3-dioxygenase 2 controls m2 macrophages polarization to promote esophageal squamous cell

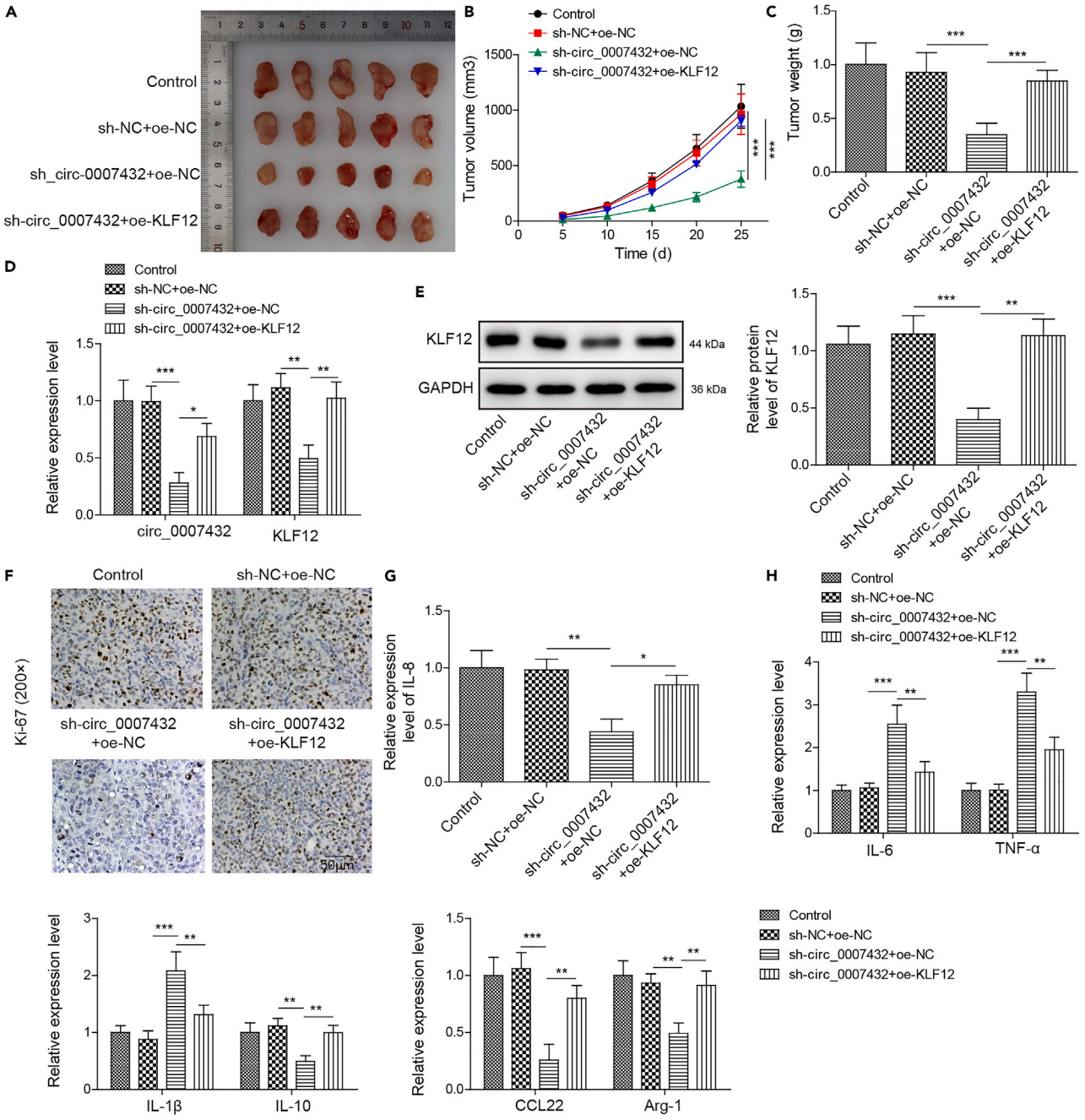

Figure 7. Circ_0007432 promoted tumorigenesis in mice and M2 macrophage polarization by affecting KLF12

A549 cells stably transfected with sh-circ_0007432 or together with oe-KLF12 were injected subcutaneously into mice.

(A) Tumor image.

(B) Tumor growth curve.

(C) Tumor weight.

(D) Circ_0007432 and KLF12 expression was detected using RT-qPCR.

(E) KLF12 protein expression was examined using western blot.

(F) Ki67 was measured by IHC. Scale bar: 50 μm.

(G) IL-8 expression was detected using RT-qPCR.

(H) IL-6, TNF-α, IL-1β, IL-10, CCL22, and Arg-1 levels in THP-1 cells were detected by RT-qPCR. $n = 5$. Data were shown as mean ± SD. Each experiment was accomplished in triplicates. *$p < 0.05$, **$p < 0.01$, ***$p < 0.001$. One-way analysis of variance (ANOVA) for (B), (C), (D), (E), (G), and (H).

carcinoma progression via akt/gsk3β/il-8 signaling pathway. Acta Pharm. Sin. B *11*, 2835–2849.
24. Yan, P., Zhu, H., Yin, L., Wang, L., Xie, P., Ye, J., Jiang, X., and He, X. (2018). Integrin αvβ6 promotes lung cancer proliferation and metastasis through upregulation of il-8-mediated mapk/erk signaling. Transl. Oncol. *11*, 619–627.
25. Cléry, A., Krepl, M., Nguyen, C.K.X., Moursy, A., Jorjani, H., Katsantoni, M., Okoniewski, M., Mittal, N., Zavolan, M., Sponer, J., and Allain, F.H.T. (2021). Structure of srsf1 rrm1 bound to rna reveals an unexpected bimodal mode of interaction and explains its involvement in smn1 exon7 splicing. Nat. Commun. *12*, 428.
26. Liu, B., Ma, H., Liu, X., and Xing, W. (2023). Circscn8a suppresses malignant progression and induces ferroptosis in non-small cell lung cancer by regulating mir-1290/acsl4 axis. Cell Cycle *22*, 758–776.
27. Sedighzadeh, S.S., Khoshbin, A.P., Razi, S., Keshavarz-Fathi, M., and Rezaei, N. (2021). A narrative review of tumor-associated macrophages in lung cancer: Regulation of macrophage polarization and therapeutic implications. Transl. Lung Cancer Res. *10*, 1889–1916.
28. Kristensen, L.S., Jakobsen, T., Hager, H., and Kjems, J. (2022). The emerging roles of circrnas in cancer and oncology. Nat. Rev. Clin. Oncol. *19*, 188–206.
29. Curry, D.L. (1970). Glucagon potentiation of insulin secretion by the perfused rat pancreas. Diabetes *19*, 420–428.
30. Hansen, T.B., Jensen, T.I., Clausen, B.H., Bramsen, J.B., Finsen, B., Damgaard, C.K., and Kjems, J. (2013). Natural rna circles function as efficient microrna sponges. Nature *495*, 384–388.
31. Chen, R., Wang, S.K., Belk, J.A., Amaya, L., Li, Z., Cardenas, A., Abe, B.T., Chen, C.K., Wender, P.A., and Chang, H.Y. (2023). Engineering circular rna for enhanced protein production. Nat. Biotechnol. *41*, 262–272.
32. Ren, X., Yu, J., Guo, L., and Ma, H. (2021). Circular rna circrhot1 contributes to pathogenesis of non-small cell lung cancer by epigenetically enhancing c-myc expression through recruiting kat5. Aging (Albany NY) *13*, 20372–20382.
33. Wang, F., Niu, Y., Chen, K., Yuan, X., Qin, Y., Zheng, F., Cui, Z., Lu, W., Wu, Y., and Xia, D. (2023). Extracellular vesicle-packaged circatp2b4 mediates m2 macrophage polarization via mir-532-3p/srebf1 axis to promote epithelial ovarian cancer metastasis. Cancer Immunol. Res. *11*, 199–216.
34. Chen, W., Tang, D., Lin, J., Huang, X., Lin, S., Shen, G., and Dai, Y. (2022). Exosomal circshkbp1 participates in non-small cell lung cancer progression through pkm2-mediated glycolysis. Mol. Ther. Oncolytics *24*, 470–485.
35. Liu, Y., Ao, X., Yu, W., Zhang, Y., and Wang, J. (2022). Biogenesis, functions, and clinical implications of circular rnas in non-small cell lung cancer. Mol. Ther. Nucleic Acids *27*, 50–72.
36. Zhang, S., Zeng, X., Ding, T., Guo, L., Li, Y., Ou, S., and Yuan, H. (2018). Microarray profile of circular rnas identifies hsa_circ_0014130 as a new circular rna biomarker in non-small cell lung cancer. Sci. Rep. *8*, 2878.
37. Wang, J., Pu, J., Zhang, Y., Yao, T., Luo, Z., Li, W., Xu, G., Liu, J., Wei, W., and Deng, Y. (2019). Dancr contributed to hepatocellular carcinoma malignancy via sponging mir-216a-5p and modulating klf12. J. Cell. Physiol. *234*, 9408–9416.
38. Song, P., and Yin, S.C. (2019). Long non-coding rna 319 facilitates nasopharyngeal carcinoma carcinogenesis through regulation of mir-1207-5p/klf12 axis. Gene *680*, 51–58.
39. Wu, G., Zhang, A., Yang, Y., and Wu, D. (2021). Circ-rnf111 aggravates the malignancy of gastric cancer through mir-876-3p-dependent regulation of klf12. World J. Surg. Oncol. *19*, 259.
40. Nasiri-Aghdam, M., Garcia-Garduño, T.C., and Jave-Suárez, L.F. (2021). Celf family proteins in cancer: Highlights on the rna-binding protein/noncoding rna regulatory axis. Int. J. Mol. Sci. *22*, 11056.
41. Wang, B., Chen, H., Deng, Y., Chen, H., Xing, L., Guo, Y., Wang, M., and Chen, J. (2023). Circdnajc11 interacts with taf15 to promote breast cancer progression via enhancing mapk6 expression and activating the mapk signaling pathway. J. Transl. Med. *21*, 186.
42. Howard, J.M., and Sanford, J.R. (2015). The rnaissance family: Sr proteins as multifaceted regulators of gene expression. Wiley Interdiscip. Rev. RNA *6*, 93–110.
43. Yang, M., Wang, W., Wang, L., and Li, Y. (2023). Circ_0001052 promotes cardiac hypertrophy via elevating hipk3. Aging (Albany NY) *15*, 1025–1038.
44. Chan, J.H.P., Lim, S., and Wong, W.S.F. (2006). Antisense oligonucleotides: From design to therapeutic application. Clin. Exp. Pharmacol. Physiol. *33*, 533–540.
45. Gleave, M.E., and Monia, B.P. (2005). Antisense therapy for cancer. Nat. Rev. Cancer *5*, 468–479.
46. Welters, I.D., Hafer, G., Menzebach, A., Mühling, J., Neuhäuser, C., Browning, P., and Goumon, Y. (2010). Ketamine inhibits transcription factors activator protein 1 and nuclear factor-kappab, interleukin-8 production, as well as cd11b and cd16 expression: Studies in human leukocytes and leukocytic cell lines. Anesth. Analg. *110*, 934–941.
47. Xiao, P., Long, X., Zhang, L., Ye, Y., Guo, J., Liu, P., Zhang, R., Ning, J., Yu, W., Wei, F., and Yu, J. (2018). Neurotensin/il-8 pathway orchestrates local inflammatory response and tumor invasion by inducing m2 polarization of tumor-associated macrophages and epithelial-mesenchymal transition of hepatocellular carcinoma cells. OncoImmunology *7*, e1440166.
48. Zhang, W., Yang, F., Zheng, Z., Li, C., Mao, S., Wu, Y., Wang, R., Zhang, J., Zhang, Y., Wang, H., et al. (2022). Sulfatase 2 affects polarization of m2 macrophages through the il-8/jak2/stat3 pathway in bladder cancer. Cancers *15*, 131.
49. Quail, D.F., and Joyce, J.A. (2013). Microenvironmental regulation of tumor progression and metastasis. Nat. Med. *19*, 1423–1437.
50. Mantovani, A., Marchesi, F., Malesci, A., Laghi, L., and Allavena, P. (2017). Tumour-associated macrophages as treatment targets in oncology. Nat. Rev. Clin. Oncol. *14*, 399–416.

STAR★METHODS

KEY RESOURCES TABLE

REAGENT or RESOURCE	SOURCE	IDENTIFIER
Antibodies		
Rabbit monoclonal anti-Bax	Abcam	Cat# ab32503; RRID:AB_725631
Rabbit monoclonal anti-Bcl-2	Abcam	Cat# ab182858; AB_2715467
Rabbit polyclonal anti-KLF12	Thermo Fisher Scientific	Cat# PA5-120729; AB_2914301
Rabbit polyclonal anti-SRSF1	Proteintech	Cat# 12929-2-AP; AB_2187211
Rabbit monoclonal anti-IL-8	Abcam	Cat# ab289967; AB_2933977
Rabbit monoclonal anti-GAPDH	CST	Cat# 5174S; AB_10622025
Rabbit monoclonal HRP-labeled secondary antibody	Abcam	Cat# ab181236
Rabbit monoclonal anti-Ago2	Abcam	Cat# ab186733; AB_2713978
Rabbit polyclonal anti-SRSF1	Abcam	Cat# ab38017; AB_882519
Rabbit polyclonal anti-IgG	Proteintech	Cat# 30000-0-AP; AB_2819035
Biological samples		
Human NSCLC tumor tissues and paired-para-cancer tissues	Hainan Medical University	N/A
Chemicals, peptides, and recombinant proteins		
PMA	Sigma-Aldrich	Cat# 16561-29-8
TRIzol reagent	Beyotime	Cat# R0011
ECL chemiluminescent reagent	Beyotime	Cat# P0018S
DAB	Beyotime	Cat# P0202
Actinomycin D	Merck	Cat# SBR00013
DNase I	Solarbio	Cat# D8071
Critical commercial assays		
ELISA kits	Thermo Fisher Scientific	Cat# BMS204-3
Script Reverse Transcription Reagent Kit	TaKaRa	Cat# 6110A
SYBR Premix Ex Taq II Kit	TaKaRa	Cat# RR820B
PARIS™ Kit	Invitrogen	Cat# AM1921
Annexin V-FITC apoptosis detection kit	Beyotime	Cat# C1062S
BCA protein quantitative kit	Thermo Fisher Scientific	Cat#23227
Pierce™ Magnetic ChIP Kit	Thermo Fisher Scientific	Cat# 26157
PierceTM Magnetic RNA-Protein Pull-Down kit	Sigma-Aldrich	Cat# 20164
A Magna RIP Kit	Sigma-Aldrich	Cat# 17-700
the chemiluminescence EMSA kit	Thermo Fisher Scientific	Cat# 20158
Deposited data		
Raw data	This paper	URL: https://osf.io/syd68/; https://doi.org/10.17605/OSF.IO/SYD68
Experimental models: Cell lines		
Human: H358	ATCC	Cat# CRL-5807
Human: PC-9	Icell	Cat# h263

(*Continued on next page*)

Continued

REAGENT or RESOURCE	SOURCE	IDENTIFIER
Human: H1975	ATCC	Cat# CRL-5908
Human: Calu-3	ATCC	Cat# HTB-55
Human: A549	ATCC	Cat# CRM-CCL-185
Human: BEAS-2B	ATCC	Cat# CRL-3588
Human: THP-1	ATCC	Cat# TIB-202
Human: 293T	ATCC	Cat# CRL-3216
Experimental models: Organisms/strains		
Mouse: BALB/c nude mice	Slac Jingda Laboratory Animal Co., Ltd.	N/A
Oligonucleotides		
sh-circ_0007432	GenePharma	N/A
sh-SRSF1	GenePharma	N/A
sh-NC	GenePharma	N/A
oe-KLF12	GenePharma	N/A
oe-circ_0007432	GenePharma	N/A
oe-NC	GenePharma	N/A
Biotin labeled circ_0007432 probes	GenePharma	N/A
Software and algorithms		
ImageJ	N/A	https://imagej.nih.gov/ij/
JASPAR	N/A	http://jaspar.genereg.net/

RESOURCE AVAILABILITY

Lead contact

Further information about data, resources and reagents should be obtained by contacting the corresponding author Jinsheng Wu.

Materials availability

The plasmids, cell lines, experimental animals, and other reagents are commercially available and can be purchased from the corresponding suppliers.

Data and code availability

All data generated or analyzed in this study are included in this published article. All data reported in this paper will be shared by the lead contact upon request. Any additional information necessary to reanalyze the data reported in this paper is available upon request from the lead. This article does not report original code.

EXPERIMENTAL MODEL AND STUDY PARTICIPANT DETAILS

Tumor tissues and Paired-para-cancer tissues from NSCLC patients (50 cases) were collected from The First Affiliated Hospital of Hainan Medical University. All cases were confirmed by clinical and pathological diagnosis without any drug treatment before sampling. The collected tissues were stored at −80°C. All cases were confirmed by clinical and pathological diagnosis without any drug treatment before sampling. Our study was approved by the Ethics Committee of The First Affiliated Hospital of Hainan Medical University. All participants were signed the informed consent.

The cells lines including BEAS-2B, A549, Calu-3, H1975, H358, THP-1 and 293T were bought from ATCC (USA). PC-9 cells line was bought from iCell (China). All cells involved in this study were authenticated by Short tandem repeats (STR) and were confirmed to be free of mycoplasma contamination by PCR and culture. Cells were maintained in DMEM (Thermo Fisher Scientific, USA) with 10% FBS (Thermo Fisher Scientific) and 1% antibiotics (Beyotime, Shanghai, China) under the condition of 5% CO_2 and 37°C.

Animal experiments were approved by the ethics committee of The First Affiliated Hospital of Hainan Medical University. BALB/c nude mice (male, 3-5 weeks of age) were obtained from Slac Jingda Laboratory Animal Co., Ltd. (Hunan, China). Under the appropriate temperature and humidity, mice maintained a 12 h circadian rhythm and freely ate and drank water. After one week of adaptive feeding, it was used in the experiment.

METHOD DETAILS

Co-culture system of THP-1 cells and NSCLC cells

A transwell chamber (Corning, USA) was applied for cocultivation system of THP-1 cells and NSCLC cells. THP-1 cells were placed in the lower and were treated with 100 ng/mL 12-*O*-tetradecanoylphorbol-13-acetate (16561-29-8, PMA, Sigma-Aldrich) for 48 h to induce macrophages. In addition, NSCLC cells were placed in the upper chamber. THP-1 cells after PMA treatment were co-cultured with A549 or H1975 cells transfected with indicated designs.

Cell transfection

To knockdown circ_0007432 and SRSF1 in A549 and H1975 cells, lentivirus carrying the short hairpin RNA targeting circ_0007432 (sh-circ_0007432), SRSF1 (sh-SRSF1) and KLF12 (sh-KLF12) were employed to infect NSCLC cells. In addition, to overexpress KLF12 and circ_0007432, lentivirus carrying overexpression vector of KLF1 (oe-KLF12) and circ_0007432 (oe-circ_0007432) were transfected into NSCLC cells. In addition, lentiviruses containing empty plasmids (vector) were used as controls. The above lentivirus was obtained from GenePharma (China). Cells were seeded into a T25 culture flask separately, cultured overnight. Then, 2 mL of culture medium without penicillin/streptomycin was added to each bottle. Lentivirus was directly added to the culture medium. After 16 h, the medium containing lentivirus was discarded and replaced with new complete medium. After 72 h, puromycin was added to the medium for one week to screen stably infected cells.

RNase R digestion

To detect the degradation of circ_0007432 and PMM2 mRNA, the collected RNAs of H1975 and A549 cells were treated with RNase R (3 U/μg, Sigma-Aldrich, USA) for 1 h at 37°C. Then, RT-qPCR was conducted and the levels of circ_0007432 and PMM2 mRNA were evaluated. The detailed procedure of RT-qPCR could be found in RT-qPCR in the STAR Methods section.

RNA stability

To detect RNA stability of KLF12. Actinomycin D (2 μg/mL, SBR00013, Merck, USA) was added to block gene transcription process of cells. Then, RT-qPCR was used to evaluate KLF12 mRNA level after 0, 2, 4, 6 and 8 h.

RT-qPCR

Total RNAs extracted from cells or tumor tissues were extracted using TRIzol reagent (R0011, Beyotime, China). RNA concentration and the optical density (OD) value were measured with the Nano-500 microspectrophotometer (Allsheng, Hangzhou, China). 1 μg RNA was used to synthesize cDNA using Script Reverse Transcription Reagent Kit (6110A, TaKaRa, Japan). qPCR process was implemented by SYBR Premix Ex Taq II Kit (RR820B, TaKaRa) in the ABI StepOne Real-time Detection System (LTC, Carlsbad, USA). The thermal cycling conditions were as follows: 95°C for 5 min, 90°C for 15 s, 60°C for 45 s, repeating for 40 cycles. The primer sequences were presented in below table. The relative expression of targeted genes was calculate using $2^{-\Delta\Delta Ct}$ formula. GAPDH served as reference gene.

The primer sequences

Genes	Forward sequences	Reverse sequences
circ_0007432	5′-GCGACATGTGGAAAATGACGG -3′	5′-TGCTACCAAGCCATTTTCTGG -3′
SRSF1	5′-CCGCAGGGAACAACGATTG -3′	5′-GCCGTATTTGTAGAACACGTCCT-3′
KLF12	5′-CGGCAGTCAGAGTCAAAACAG-3′	5′-CGGCTTCCATATCGGGATAGT-3′
IL-8	5′-CACAAGAGCCAGGAAGAAAC-3′	5′-CTACAACAGACCCACACAATAC-3′
IL-6	5′-TACCCCCAGGAGAAGATTCC-3′	5′-TACCCCCAGGAGAAGATTCC-3′
TNF-α	5′-CCCAGGGGACCTCTCTCTAATC-3′	5′-ATGGGCTACAGGCTTGTCACT-3′
IL-1β	5′-CGATGCACCTGTACGATCAC-3′	5′-TCTTTCAACACGCAGGACAG-3′
IL-10	5′-GCCAAGCCTTGTCTGAGATG-3′	5′-GGCCTTGCTCTTGTTTTCAC-3′
CCL22	5′-ATGGATCGCCTACAGACTGC-3′	5′-CGGCACAGATCTCCTTATCC-3′
Arg-1	5′-GTGGAAACTTGCATGGACAAC-3′	5′-AATCCTGGCACATCGGGAATC-3′
GAPDH	5′-CCAGGTGGTCTCCTCTGA-3′	5′-GCTGTAGCCAAATCGTTGT-3′

Fluorescence *in situ* hybridization (FISH)

To detect the location of circ_0007432 in H1975 and A549 cells, FISH assay was conducted. Cy5-labelled circ_0007432 probe was synthesized by Servicebio (China). Then, circ_0007432 probe was applied to incubate samples. DAPI stained cell nuclei. Fluorescence intensity was examined using a fluorescence microscope (Olympus, Japan).

Nuclear/cytoplasmic fractionation

NSCLC cells were washed twice before cell scraping. Nuclear and cytoplasmic RNAs of H1975 and A549 cells were separated using PARIS Kit (Invitrogen, USA). Cytoplasmic lysis buffer was added in suspend cell pellet. Cells were lysed for 3 min on ice. After centrifugation, supernatant was collected as the cytosol fraction. Pellet was washed by 0.5 × TBS with 0.1% NP-40 twice and then lysed with nuclear lysis buffer for 10 min on ice. After centrifugation, the supernatant was collected as the nuclear fraction. After purification and DNase I (D8071, Solarbio, China) treatment, nuclear and cytoplasmic RNAs were reverse-transcribed into cDNAs. The expression of circ_0007432, GAPDH and U6 was detected by RT-qPCR.

Cell counting kit-8 (CCK-8) assay

A549 or H1975 cells (1×10^3 cells/well) with indicated transfection were implanted onto 96-well plates for overnight. Next, 10 μL CCK-8 solution (Beyotime) was added to each well. After incubation for 2 h, the absorbance at 450 nm was examined by a microplate reader (Thermo Fisher Scientific).

Flow cytometry

To detect cell apoptosis, flow cytometry was applied. Shortly, around 2×10^6 cells were collected and the cells were cultured with 10 μL Annexin V-FITC (C1062S-1, Beyotime) and 5 μL PI (C1062S-3, Beyotime) stain in the dark. After incubation for 10 min, samples were immediately analyzed using flow cytometry.

After PMA treatment, THP-1 cells were co-cultured with A549 or H1975 cells transfected with sh-circ_0007432 or in combination with oe-KLF12. Then, cells were subjected to incubation with fluorescence-conjugated antibodies against phycoerythrin (PE) CD86 and FITC CD206 in PBS for 30 min at 4°C. A flow cytometer (BD Biosciences, USA) was applied to test the surface markers.

Western blot

Cells and tumor tissues were lysed in RIPA buffer (Beyotime) to obtain total proteins. The exact concentration of proteins was detected using BCA protein quantitative kit (Thermo Fisher Scientific). Equivalent proteins in each sample hole (30 μg) were isolated using 10% SDS–PAGE after the protein concentration of samples was determined. After electrophoresis, the separated proteins in SDS–PAGE were transferred onto PVDF membranes in a semi-wet system. Membranes were blocked with 5% skimmed milk for 1 h at room temperature. Primary antibodies were performed for incubation of membranes overnight at 4°C. Next, the membranes were washed with 1 × TBST three times. An HRP-labeled secondary antibody (ab181236, 1:10000, Abcam, UK) was used for incubation the membranes. ECL chemiluminescent reagent (P0018S, Beyotime) was added on membranes to visualize protein bands. The gray values were obtained using ImageJ (National Institutes of Health, USA). The detailed information of primary antibodies used in this study were as follows: anti-Bax (ab32503, 1:5000, Abcam), anti-Bcl-2 (ab182858, 1:2000, Abcam), anti-KLF12 (PA5-120729, 1:2000, Thermo Fisher Scientific), anti-SRSF1 (12929-2-AP, 1:1000, Proteintech, USA), anti-IL-8 (ab289967, 1:1000, Abcam) and anti-GAPDH (5174S, 1:1000, CST, USA).

Wound healing assay

A549 or H1975 cells (1×10^4 cells/well) with different transfections were implanted on 6-well plates with cellular monolayers overnight. Then, cells were scratched with a micropipette tip. After washed using PBS solution, cells were continually cultured for 48 h. The scratched widths were measured under an optical microscope and recorded at 0 and 48 h.

Transwell assay

To examine ability of cell invasion, a 24-well transwell insert system (Corning, USA) was employed for this assay. Shortly, top transwell chamber was covered with Matrigel (Becton Dickinson Biosciences, USA). A549 or H1975 cells were seeded onto the upper chamber containing serum-free DMEM and the lower chamber was added with DMEM and 10% FBS. After 24 h, the invaded cells on the below side of chamber were fixed with 95% alcohol. 1% crystal violet (Sigma-Aldrich, USA) was performed to stain the invaded cells. An optical microscope was employed to observe invaded cells.

RNA-binding protein immunoprecipitation (RIP)

To detect whether circ_0007432 sponges miRNA and verify the interactions among circ_0007432, SRSF1 and KLF12, RIP assay was conducted using A Magna RIP Kit (17–700, Sigma-Aldrich). In brief, H1975 and A549 cells were collected and lysed using RIPA buffer. After centrifugation, the supernatant was collected and incubated with magnetic beads conjugated with anti-Ago2 (ab186733, 1:50, Abcam), anti-SRSF1 (ab38017, 1:50, Abcam) or anti-IgG (30000-0-AP, 2 μg, Proteintech) antibody for immunoprecipitation. After protein digestion with proteinase K (Sigma-Aldrich), RNA was extracted using TRIzol (TAKARA, Japan). The enrichment of the immunoprecipitated RNAs, including circ_0007432 and KLF12, was detected using RT-qPCR.

RNA pull-down assay

To validate the interaction between circ_0007432 and SRSF1, a PierceTM Magnetic RNA-Protein Pull-Down kit (Thermo Fisher Scientific) was utilized for the RNA pull-down assay. Shortly, H1975 and A549 cells were transfected with biotin-labeled probe against scramble or

circ_0007432. 48 h later, cells were incubated with lysis buffer after washing. The lysate was incubated with streptavidin-coated magnetic beads at 4°C overnight. Beads were then washed to remove RNA-binding protein complexes. The SRSF1 enrichment was measured by western blot.

RNA electrophoretic mobility shift assay (EMSA)

Biotin-labeled circular probe of circ_0007432 was generated by Genepharma (Shanghai, China). Unlabeled circ_0007432 was applied as competitor. For the EMSA assay, in brief, the biotinylated circ_0007432 and Myc-labeled SRSF1 protein were reacted in 10 mL of binding reaction buffer at room temperature for 20 min. Then, the complexes were separated using non-denaturing polyacrylamide gel electrophoresis. Biotinylated RNA was measured in the blots with a chemiluminescent RNA EMSA Kit (Thermo Fisher Scientific).

Enzyme-linked immunosorbent assay (ELISA)

A549 or H1975 cells received indicated transfection were seeded into 96-well plates at a density of 1×10^4 cells per well for 24 h and then the supernatants were collected and centrifuged. The concentrations of IL-8 in supernatants were examined using ELISA kits (BMS204-3, Thermo Fisher Scientific) according to Manufacturer's instructions.

Chromatin immunoprecipitation (ChIP) assay

To validate the interaction between KLF12 and IL-8 promoter, ChIP assay was conducted using the Pierce Magnetic ChIP Kit (Thermo Fisher Scientific). H1975 and A549 cells underwent cross-linking reaction with 1% paraformaldehyde and then were terminated by the addition of 0.125 M glycine. Then, cells were harvested by scraping and the resulting cell pellets were disrupted. Nuclei were collected using a membrane extraction buffer, digested with micrococcal nuclease and lysed by sonication to obtain chromatin 200–800 bp fragments. The fragments were incubated with the primary antibody KLF12 or Ig G at 4°C overnight. Protein A/G magnetic beads were added to the antibody-chromatin complex and mixed for 2 h. RNase A and proteinase K were used to reverse crosslink the chromatin samples. The immunoprecipitated DNA was analyzed using PCR after washing and purification.

Dual luciferase reporter assay

The wild-type and mutant IL-8 promoter sequences (WT-IL-8: 5′-GGGGATG-3′, MUT-IL-8: 5′-GCCCAAG-3′) were cloned into a psiCheck2 vector (Promega, WI, USA). WT-IL-8/MUT-IL-8 and sh-KLF12 were co-transfected into H1975 and A549 cells using Lipofectamine 3000 Reagent (Invitrogen). Luciferase activity was evaluated using dual luciferase reporter assay system (Promega).

Tumor formation in nude mice

Nude mice (male, 3–5 weeks of age) were randomly divided into four groups with 5 mice in each group. The investigators were blinded to grouping assignment. After infected with lentivirus carrying sh-circ_0007432 or in combination with oe-KLF12, A549 cells (1×10^6 cells) were inoculated into the subcutaneous axilla of the left forelimb of nude mice. Tumor volume was then measured every 5 days until day 25. Then, mice were euthanized and tumor tissues were completely removed. Tumor tissues were used for immunohistochemistry (IHC), RT-qPCR or western blot. Animal experiments were approved by the ethics committee of The First Affiliated Hospital of Hainan Medical University.

Immunohistochemical (IHC) staining

IHC was performed to determine Ki67 protein expression in tumor tissues. In short, tumor tissues were fixed using 4% paraformaldehyde for 24 h and embedded in paraffin. Roughly 5 μm sections were prepared. The paraffin sections were baked at 60°C for 2 h and dewaxed in fresh xylene for 30 min. Then, the slides were hydrated with gradient alcohol, followed by boiling them in a pressure cooker containing sodium citrate for 2 min to retrieve the antigens. Next, sections cooled to room temperature were incubated with an endogenous peroxidase blocking agent for 15 min and blocked with 1% BSA for 20 min. The sections were incubated with primary antibody against Ki67 (Abcam) overnight at 4°C. After washing with PBS buffer, the sections were incubated with HRP-labelled antibody. The sections were counterstained with diaminobenzidine (DAB, P0202, Beyotime). Finally, the images were observed under an optical microscope (Olympus).

QUANTIFICATION AND STATISTICAL ANALYSIS

All data were presented as means ± standard deviation (SD). The normality of data was assessed by the Shapiro-Wilk test. Considering a significance level of 5%, there were no significant deviations from the normality of all data ($p > 0.05$). All the *in vitro* results were three separate experiments performed in triplicate. Using GraphPad Prism 9 analyzed all data. Student's t test and one-way analysis of variance (ANOVA) were applied to conduct comparison of groups. The correlations between circ_0007432 and overall survival in NSCLC patients was analyzed using Kaplan-Meier survival analysis. The interaction of genes was analyzed using Pearson correlation analysis. $p < 0.05$ was regarded as statistically significant difference. $^*p < 0.05$, $^{**}p < 0.01$, $^{***}p < 0.001$.